

Asymmetric Leptoquark Pair Production at LHC

Ilja Doršner,^{a,b} Ajla Lejlić,^c Shaikh Saad^d

^a*University of Split, Faculty of Electrical Engineering, Mechanical Engineering and Naval Architecture in Split, Ruđera Boškovića 32, HR-21000 Split, Croatia*

^b*J. Stefan Institute, Jamova 39, P. O. Box 3000, SI-1001 Ljubljana, Slovenia*

^c*Department of Physics, Faculty of Science, University of Zagreb, Bijenička cesta 32, HR-10000 Zagreb, Croatia*

^d*Department of Physics, University of Basel, Klingelbergstrasse 82, CH-4056 Basel, Switzerland*

E-mail: dorsner@fesb.hr, ajla@me.com, shaikh.saad@unibas.ch

ABSTRACT: We investigate asymmetric leptoquark pair production mechanism at the Large Hadron Collider to advocate its potential relevance to establish reliable constraints on the leptoquark parameter space and its ability to aid in correct identification of these attractive sources of new physics. The main feature of asymmetric pair production that genuinely distinguishes it from the usual leptoquark pair production is given by the fact that the two leptoquarks that are produced in proton-proton collisions through a t -channel lepton exchange are not charge conjugates of each other. Hence the proposed name of asymmetric leptoquark pair production for this type of process. We spell out prerequisite conditions for the asymmetric leptoquark pair production mechanism to be operational and enumerate all possible combinations of leptoquark multiplets that can potentially generate it. We finally reinterpret existing leptoquark pair production search results within several simple scalar leptoquark extensions of the Standard Model, assuming that the leptoquarks exclusively couple to either electrons or muons and the first generation quarks, to demonstrate proper inclusion of asymmetric pair production. We consequently present accurate parameter space constraints for the S_1 , S_3 , R_2 , S_1+S_3 , and S_1+R_2 leptoquark scenarios.

Contents

1	Introduction	1
2	Asymmetric pair production	4
2.1	Case studies	10
2.1.1	Case study: $S_1(\bar{\mathbf{3}}, \mathbf{1}, 1/3)$	11
2.1.2	Case study: $R_2(\mathbf{3}, \mathbf{2}, 7/6)$	13
2.1.3	Case study: $S_1(\bar{\mathbf{3}}, \mathbf{1}, 1/3) + R_2(\mathbf{3}, \mathbf{2}, 7/6)$	16
2.1.4	Case study: $S_3(\bar{\mathbf{3}}, \mathbf{3}, 1/3)$	18
2.1.5	Case study: $S_1(\bar{\mathbf{3}}, \mathbf{1}, 1/3) + S_3(\bar{\mathbf{3}}, \mathbf{3}, 1/3)$	19
2.2	Final remarks	22
3	Atomic parity violation	22
4	Conclusions	26

1 Introduction

Leptoquark pair production is the only available process to efficiently look for these hypothetical particles at hadron colliders when the coupling strength between the relevant quark-lepton pairs and a leptoquark is small. It is thus clear that the search for leptoquarks via pair production is always going to be an integral part of the Large Hadron Collider (LHC) experimental agenda in years, if not decades, to come. (For a sample of the leptoquark pair production search results, see Refs. [1–5].) The leptoquark pair production cross sections applicable to LHC are accordingly available at the next-to-leading order [6–9] as well as the next-to-next-to-leading order [10–13] in strong coupling constant, and, more recently, at the next-to-leading order in both the strong coupling constant and the leptoquark Yukawa coupling(s) [14].

As the strength of interaction between the quark-lepton pairs and a leptoquark is gradually increased, the collider searches for signals from several other processes start to be relevant in constraining the leptoquark parameter space. These processes, at the LHC, are a single leptoquark production [9, 15–19], a non-resonant production of the Drell-Yan type [19–25], and a resonant leptoquark production [26–30].

Note, however, that even the leptoquark pair production exhibits dependence on the Yukawa coupling strength [16]. This is especially true in the case of a novel mechanism of leptoquark pair production that has been recently introduced in Ref. [31]. The main feature of this novel mechanism that distinguishes it from the usual leptoquark pair production at the LHC is the fact that the two leptoquarks that are produced in proton-proton collisions through a t -channel exchange of a lepton do not comprise a charge conjugate pair. This

$(SU(3), SU(2), U(1))$	LQ SYMBOL	CHIRALITY TYPE (LQ- q - l)	F
$(\bar{\mathbf{3}}, \mathbf{3}, 1/3)$	S_3	LL	-2
$(\mathbf{3}, \mathbf{2}, 7/6)$	R_2	RL, LR	0
$(\mathbf{3}, \mathbf{2}, 1/6)$	\tilde{R}_2	RL	0
$(\bar{\mathbf{3}}, \mathbf{1}, 4/3)$	\tilde{S}_1	RR	-2
$(\bar{\mathbf{3}}, \mathbf{1}, 1/3)$	S_1	LL, RR	-2

Table 1. Scalar leptoquark multiplets, chiralities of the leptoquark interactions with the SM quark-lepton pairs, and associated leptoquark fermion numbers.

is a primary reason why we refer to it as an asymmetric leptoquark pair production in this study. The novel production mechanism, though, can yield the same final state as the conventional pair production. In fact, the final state kinematics should be exactly the same if the leptoquarks in question are degenerate in mass. This work aims to address the correct interpretation of existing and future experimental search results for those final states that are due to the leptoquark pair production processes and subsequent leptoquark decays if one appropriately incorporates the aforementioned asymmetric mechanism contributions. It dovetails the initial analysis of Ref. [31] and extends the scope of the phenomenological discussion of asymmetric pair production presented therein. It also nicely complements recent work on the inclusion of the asymmetric pair production mechanism in the next-to-leading order in QCD cross section determinations for the leptoquark pair production [32]. We stress that the asymmetric contributions to the leptoquark pair production have not been included in any of publicly available experimental search analyses thus far.

We will, for definiteness, focus our attention solely on the scalar leptoquark extensions of the Standard Model (SM). We accordingly present in Table 1 a list of pertinent scalar leptoquarks and associated transformation properties under the SM gauge group $SU(3) \times SU(2) \times U(1)$. Since the chirality of the leptons that the scalar leptoquark couples to is very important for our discussion, we indicate relevant chiralities of both quarks and leptons using R and L for right- and left-chiral fields, respectively, in the third column of Table 1. Our convention is such that the first (second) letter, in that column, denotes chirality of quarks (leptons). For example, the fact that S_1 leptoquark can directly couple to the $SU(2)$ doublets of quarks and leptons or/and the $SU(2)$ singlets of quarks and leptons is indicated by simultaneous presence of LL and RR designations in the third column of Table 1. We also specify fermion number F of scalar leptoquark multiplets in Table 1, where F is defined as the sum of the lepton number and three times the baryon number of leptons and quarks that a given leptoquark couples to. Leptoquarks with $F = -2$ exclusively couple/decay to quarks and leptons whereas $F = 0$ leptoquarks couple/decay to quark-antilepton or antiquark-lepton pairs.

Since our hyper-charge normalization is $Q = I_3 + Y$, where Q corresponds to electric charge in units of the positron charge, I_3 stands for the diagonal generator of $SU(2)$, and Y represents $U(1)$ hyper-charge operator, the electric charge eigenvalues of scalar leptoquarks in Table 1 are $S_3^{+4/3}$, $S_3^{+1/3}$, $S_3^{-2/3}$, $R_2^{+5/3}$, $R_2^{+2/3}$, $\tilde{R}_2^{+2/3}$, $\tilde{R}_2^{-1/3}$, $\tilde{S}_1^{+4/3}$, and $S_1^{+1/3}$. We will always denote leptoquarks using this notation and furthermore write, for simplicity,

that $(LQ^{+Q})^* = LQ^{-Q}$ and $(LQ^{-Q})^* = LQ^{+Q}$. Note that leptoquarks of the same electric charge can, in principle, mix with each other upon the breaking of the SM symmetry down to $SU(3) \times U(1)_{\text{em}}$ even if they have different fermion numbers. This type of mixing can lead to interesting physical phenomena that are somewhat orthogonal to our study. This is the main reason why we neglect all such possible mixings terms.

There are several prerequisite conditions for the asymmetric leptoquark pair production mechanism under consideration to be operational [31]. First, it requires non-negligible Yukawa coupling(s) between leptoquarks and the SM quarks and leptons. Second, this mechanism is relevant whenever there exist at least two leptoquark states originating from the same or two different leptoquark multiplets that couple to a lepton of the same chirality and flavor. This, then, leads to a simple schematic representation shown in Fig. 1 of all possible minimal leptoquark combinations that can potentially generate asymmetric pair production at hadron colliders and, consequentially, LHC.

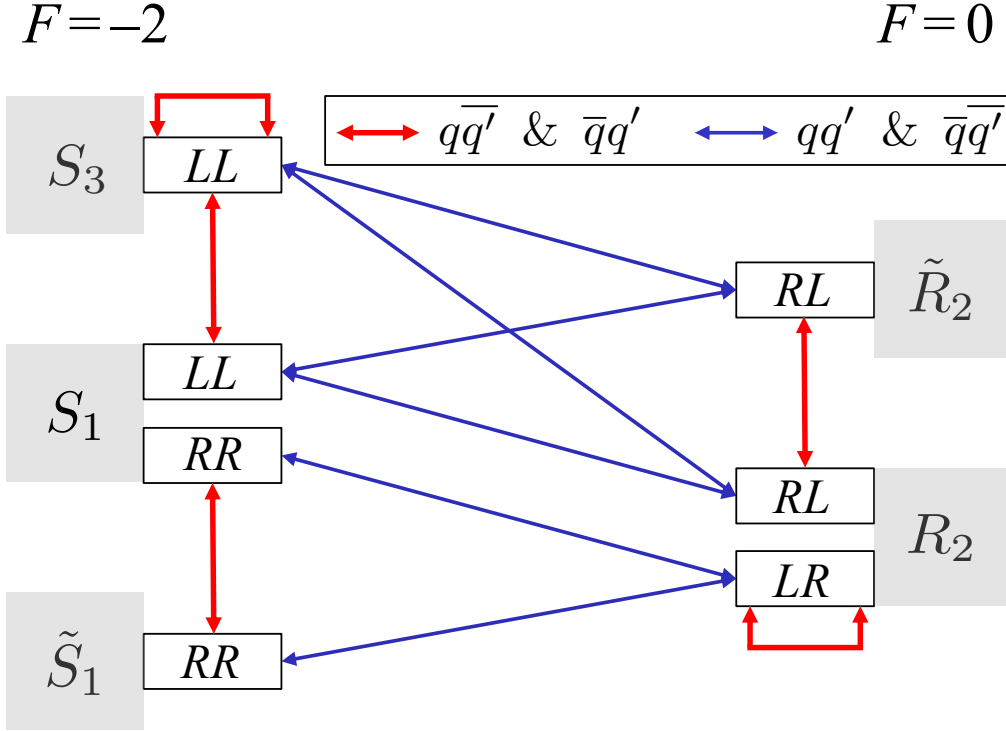


Figure 1. Schematic classification of potential sources of asymmetric leptoquark pair production. See text for details.

The double-headed arrows in Fig. 1 connect those leptoquark multiplets that can simultaneously couple to a lepton of the same flavor and chirality. For example, R_2 can couple to the SM leptons of both chiralities [33] as indicated with the RL and LR designations in Fig. 1 and Table 1. Again, it is the second letter that denotes the lepton chirality. If R_2 couples to the left-chiral leptons, it can, in principle, participate in the asymmetric pair production with all those multiplets that can also couple to the left-chiral leptons such as S_3 , S_1 , and \tilde{R}_2 . If R_2 couples to the right-chiral leptons, it can potentially contribute to

asymmetric pair production on its own, as indicated in Fig. 1, and/or in conjunction with S_1 and \tilde{S}_1 .

The double-headed arrows in Fig. 1 are color-coded either blue or red to distinguish between two different initial state configurations behind the relevant asymmetric pair production processes even though the leptoquark pairs in question are always generated in proton-proton collisions via a t -channel lepton exchange. If the two leptoquarks LQ_1 and LQ_2 have different fermion numbers, i.e., $\Delta F = |F(LQ_1)| - |F(LQ_2)| = \pm 2$, the initial states are of the qq' and $\bar{q}\bar{q}'$ nature, where q and q' denote the quark fields and can, in principle, be equal to u, d, s, c , and b . These scenarios are indicated with blue double-headed arrows in Fig. 1. If, on the other hand, leptoquarks have the same fermion number, i.e., $\Delta F = 0$, the initial states are of the $q\bar{q}'$ and $\bar{q}q'$ nature, where, again, $q, q' = u, d, s, c, b$. The $\Delta F = 0$ scenarios are depicted with red double-headed arrows in Fig. 1. In view of all these requirements, we note that it is entirely possible to have a new physics scenario with only one scalar leptoquark multiplet and only one non-zero Yukawa coupling and still be able to asymmetrically produce leptoquark pairs at the LHC [31]. There are two such scenarios, as indicated in Fig. 1. One is generated if a single non-zero Yukawa coupling exists between R_2 and any right-chiral charged lepton. The other one requires presence of a single non-zero Yukawa coupling for S_3 .

It is possible to succinctly depict all the relevant diagrams that result in asymmetric pair production at hadron colliders. There are, all in all, six such t -channel diagrams that can potentially generate asymmetric pair production. We present these diagrams in Fig. 2 and then summarize in Tables 2 and 3 associated scenarios that require presence of, at most, two scalar leptoquark multiplets when $\Delta F = 0$ and $\Delta F = \pm 2$, respectively.

The schematics in Fig. 1, diagrams of Fig. 2, and Tables 2 and 3 give a complete classification of the asymmetric pair production processes at hadron colliders. With this exhaustive classification completed we turn our attention towards more quantitative discussion of aforementioned mechanism.

The rest of the manuscript is organised as follows. In Sec. 2 we address subtleties associated with both the asymmetric and conventional leptoquark pair productions and present several specific instances of inclusion of asymmetric pair production into the usual search strategy for leptoquarks, assuming that the leptoquarks in question exclusively couple to either electrons or muons and the first generation quarks. We consequently present accurate parameter space constraints for the S_1, S_3, R_2, S_1+S_3 , and S_1+R_2 leptoquark scenarios, where, for the electron coupling case, we generate in Sec. 3 the latest limits from the atomic parity violation (APV) searches. We briefly conclude in Sec. 4.

2 Asymmetric pair production

Asymmetric pair production mechanism we want to investigate produces two leptoquarks LQ_1 and LQ_2 that are not charge conjugates of each other through one or more of the t -channel diagrams of Fig. 2. There is thus no interference between the asymmetric and conventional leptoquark pair productions at the amplitude level even though the final state signatures of both processes, upon the LQ_1 and LQ_2 subsequent decays, can be exactly the

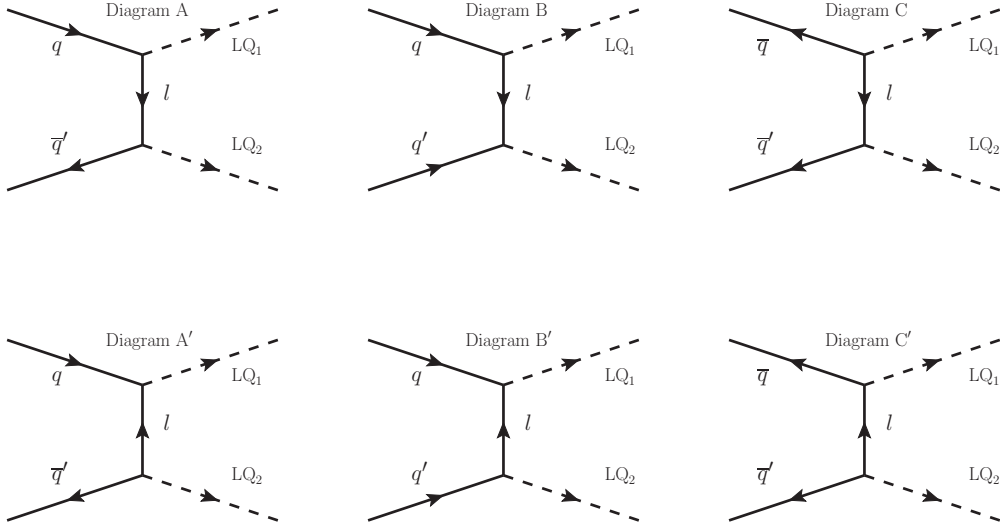


Figure 2. Types of diagrams for asymmetric production. q , q' , l , LQ_1 , and LQ_2 for $\Delta F = |F(LQ_1) - F(LQ_2)| = \pm 2$ and $\Delta F = |F(LQ_1)| - |F(LQ_2)| = 0$ are specified in Tables 2 and 3, respectively. Here l refers to a charged lepton or a neutrino.

same. We can accordingly focus our attention solely on the asymmetric pair production cross sections that can be simply added, if and when appropriate, to the conventional pair production cross sections. We work, for simplicity, at the leading order in QCD and denote the cross sections of interest with

$$\sigma_{q_1 q_2}^{\text{pair}}(y_{q_1}, y_{q_2}, m_{LQ_1}, m_{LQ_2}) = a_{q_1 q_2}(m_{LQ_1}, m_{LQ_2}) |y_{q_1} y_{q_2}|^2, \quad (2.1)$$

where $q_1, q_2 = u, \bar{u}, d, \bar{d}, s, \bar{s}, c, \bar{c}, b, \bar{b}$. Here, leptoquark LQ_i of mass m_{LQ_i} couples to a quark q_i and a lepton l of a given chirality and flavor with strength y_{q_i} , where $i = 1, 2$.

Note that the cross sections of Eq. (2.1) do not depend on whether LQ_1 couples to a quark q_1 while LQ_2 couples to a quark q_2 or vice versa. This is only relevant for subsequent leptoquark decays. The cross sections of Eq. (2.1) also do not depend on the type of lepton that leptoquarks LQ_1 and LQ_2 simultaneously couple to. They are proportional to a square of the product $|y_{q_1} y_{q_2}|$ and can thus be trivially rescaled as a function of Yukawa couplings once they are determined for one particular value of $|y_{q_1} y_{q_2}|$ product.

We will make an assumption that LQ_1 and LQ_2 are mass-degenerate, i.e., $m_{LQ_1} = m_{LQ_2} \equiv m_{LQ}$, and furthermore take all Yukawa couplings to be real. These two assumptions allow us to introduce cross section $\sigma_{q_1 q_2}^{\text{pair}}(y_{q_1}, y_{q_2}, m_{LQ})$ that is symmetric in flavor, i.e., $\sigma_{q_1 q_2}^{\text{pair}} \equiv \sigma_{q_2 q_1}^{\text{pair}}$, where

$$\sigma_{q_1 q_2}^{\text{pair}}(y_{q_1}, y_{q_2}, m_{LQ}) = \sigma_{q_1 q_2}^{\text{pair}}(y_{q_1}, y_{q_2}, m_{LQ_1} = m_{LQ_2} \equiv m_{LQ}, m_{LQ_2}). \quad (2.2)$$

Note that the cross sections of Eq. (2.2) allow us to extract limits on the leptoquark parameter space from existing experimental searches in a straightforward fashion since

Diagram Type	q	\bar{q}'	l	LQ ₁	LQ ₂	LQ scenario
A	u_L	\bar{d}_L	ℓ_R	$R_2^{+5/3}$	$R_2^{+2/3}$	R_2
A	d_L	\bar{u}_L	ℓ_R	$R_2^{-2/3}$	$R_2^{-5/3}$	
A'	d_L	\bar{u}_L	ν_L	$S_3^{-1/3}$	$S_3^{-2/3}$	S_3
A'	u_L	\bar{d}_L	ν_L	$S_3^{+2/3}$	$S_3^{+1/3}$	
A'	d_L	\bar{u}_L	ℓ_L	$S_3^{-4/3}$	$S_3^{+1/3}$	
A'	u_L	\bar{d}_L	ℓ_L	$S_3^{-1/3}$	$S_3^{+4/3}$	
A	d_R	\bar{u}_R	ℓ_L	$\tilde{R}_2^{+2/3}$	$R_2^{-5/3}$	\tilde{R}_2+R_2
A	u_R	\bar{d}_R	ℓ_L	$R_2^{+5/3}$	$\tilde{R}_2^{-2/3}$	
A	d_R	\bar{u}_R	ν_L	$\tilde{R}_2^{-1/3}$	$R_2^{-2/3}$	
A	u_R	\bar{d}_R	ν_L	$R_2^{+2/3}$	$\tilde{R}_2^{+1/3}$	
A'	d_R	\bar{u}_R	ℓ_R	$\tilde{S}_1^{-4/3}$	$S_1^{+1/3}$	\tilde{S}_1+S_1
A'	u_R	\bar{d}_R	ℓ_R	$S_1^{-1/3}$	$\tilde{S}_1^{+4/3}$	
A'	d_L	\bar{u}_L	ν_L	$S_1^{-1/3}$	$S_3^{-2/3}$	S_1+S_3
A'	u_L	\bar{d}_L	ν_L	$S_3^{+2/3}$	$S_1^{+1/3}$	
A'	u_L	\bar{d}_L	ℓ_L	$S_1^{-1/3}$	$S_3^{+4/3}$	
A'	d_L	\bar{u}_L	ℓ_L	$S_3^{-4/3}$	$S_1^{+1/3}$	

Table 2. Asymmetric production with $q\bar{q}'$ and $\bar{q}q'$ initial states. See Fig. 2 for the diagram type.

the current analyses rely on an explicit assumption of mass degeneracy for hypothetical leptoquark pairs being produced.

There are fifteen cross sections $\sigma_{q_1q_2}^{\text{pair}}(y_{q_1}, y_{q_2}, m_{\text{LQ}})$ of interest, at the LHC, when the initial states are quark-quark pairs and twenty five when the initial states are quark-antiquark pairs. We are not interested in the cross sections that are antiquark-antiquark initiated as these are highly suppressed at the LHC although we include them for completeness in the numerical simulation once we reinterpret current leptoquark search analyses results.

The quark-quark initiated cross sections are given in Fig. 3 under the assumption that $|y_{q_1}y_{q_2}| = 1$, where $q_1 = u, d, s, c$ and $q_2 = u, d, s, c, b$, while the quark-antiquark initiated cross sections are given in Fig. 4 under the same assumption that $|y_{q_1}y_{q_2}| = 1$, but, this time around, with $q_1 = u, d, s, c$ and $q_2 = \bar{u}, \bar{d}, \bar{s}, \bar{c}, \bar{b}$. We also present in Figs. 3 and 4, for comparison purposes, conventional scalar leptoquark pair production cross section at the LHC that is evaluated under the assumption that the leptoquark Yukawa couplings are negligible but still large enough to ensure prompt leptoquark decay. This particular cross section is simply denoted with $\sigma_{\text{QCD}}^{\text{pair}}(m_{\text{LQ}})$ to stress that it is purely QCD induced and it is represented by a thick dashed black curve in both Figs. 3 and 4.

The asymmetric leptoquark pair production cross sections of Figs. 3 and 4 are extracted from the new physics scenarios of Fig. 1, where all of them are generated by the t -channel processes of Fig. 2. These scenarios are implemented using FEYNRULES [34] and subsequently imported in MADGRAPH5_AMC@NLO framework [35] to produce numerical

Diagram Type	q/\bar{q}	q'/\bar{q}'	l	LQ ₁	LQ ₂	LQ scenario
B'	d_R	u_L	ℓ_R	$\tilde{S}_1^{-4/3}$	$R_2^{+5/3}$	\tilde{S}_1+R_2
B'	d_R	\bar{d}_L	ℓ_R	$\tilde{S}_1^{-4/3}$	$R_2^{+2/3}$	
C'	\bar{u}_L	\bar{d}_R	ℓ_R	$R_2^{-5/3}$	$\tilde{S}_1^{+4/3}$	
C'	\bar{d}_L	\bar{d}_R	ℓ_R	$R_2^{-2/3}$	$\tilde{S}_1^{+4/3}$	
B	u_R	d_L	ν_L	$R_2^{+2/3}$	$S_1^{-1/3}$	S_1+R_2
B	u_R	u_L	ℓ_L	$R_2^{+5/3}$	$S_1^{-1/3}$	
B	u_L	u_R	ℓ_R	$R_2^{+5/3}$	$S_1^{-1/3}$	
B	d_L	u_R	ℓ_R	$R_2^{+2/3}$	$S_1^{-1/3}$	
C	\bar{d}_L	\bar{u}_R	ν_L	$S_1^{+1/3}$	$R_2^{-2/3}$	
C	\bar{u}_L	\bar{u}_R	ℓ_L	$S_1^{+1/3}$	$R_2^{-5/3}$	
C	\bar{u}_R	\bar{u}_L	ℓ_R	$S_1^{+1/3}$	$R_2^{-5/3}$	
C	\bar{u}_R	\bar{d}_L	ℓ_R	$S_1^{+1/3}$	$R_2^{-2/3}$	
B	d_R	u_L	ℓ_L	$\tilde{R}_2^{+2/3}$	$S_1^{-1/3}$	$S_1+\tilde{R}_2$
C	\bar{u}_L	\bar{d}_R	ℓ_L	$S_1^{+1/3}$	$\tilde{R}_2^{-2/3}$	
B	u_R	d_L	ℓ_L	$R_2^{+5/3}$	$S_3^{-4/3}$	S_3+R_2
B	u_R	u_L	ℓ_L	$R_2^{+5/3}$	$S_3^{-1/3}$	
B	u_R	d_L	ν_L	$R_2^{+2/3}$	$S_3^{-1/3}$	
C	\bar{d}_L	\bar{u}_R	ℓ_L	$S_3^{+4/3}$	$R_2^{-5/3}$	
C	\bar{u}_L	\bar{u}_R	ℓ_L	$S_3^{+1/3}$	$R_2^{-5/3}$	
C	\bar{d}_L	\bar{u}_R	ν_L	$S_3^{+1/3}$	$R_2^{-2/3}$	
B	d_R	d_L	ℓ_L	$\tilde{R}_2^{+2/3}$	$S_3^{-4/3}$	$S_3+\tilde{R}_2$
B	d_R	u_L	ℓ_L	$\tilde{R}_2^{+2/3}$	$S_3^{-1/3}$	
B	d_R	u_L	ν_L	$\tilde{R}_2^{-1/3}$	$S_3^{+2/3}$	
C	\bar{d}_L	\bar{d}_R	ℓ_L	$S_3^{+4/3}$	$\tilde{R}_2^{-2/3}$	
C	\bar{u}_L	\bar{d}_R	ℓ_L	$S_3^{+1/3}$	$\tilde{R}_2^{-2/3}$	
C	\bar{u}_L	\bar{d}_R	ν_L	$S_3^{-2/3}$	$\tilde{R}_2^{+1/3}$	

Table 3. Asymmetric production with qq' and $\bar{q}\bar{q}'$ initial states. See Fig. 2 for the diagram type.

results for m_{LQ} values between 1.6 TeV and 2.6 TeV. We exclusively use the nn231o1 PDF set [36] to generate leading order cross sections for the center-of-mass energy of proton-proton collisions set at 13 TeV, where the factorisation (μ_F) and renormalization (μ_R) scales are taken to be $\mu_F = \mu_R = m_{LQ}/2$. Note that we only quote central values for all cross sections as we are solely interested in relative strengths of various potential contributions.

One can observe from Fig. 3 that the quark-quark initiated asymmetric pair production cross sections of mass-degenerate scalar leptoquarks LQ₁ and LQ₂, i.e., when $\Delta F = |F(LQ_1)| - |F(LQ_2)| = \pm 2$ and $m_{LQ_1} = m_{LQ_2} = m_{LQ}$, can be comparable to or be even substantially larger than the QCD driven leptoquark pair production cross section at

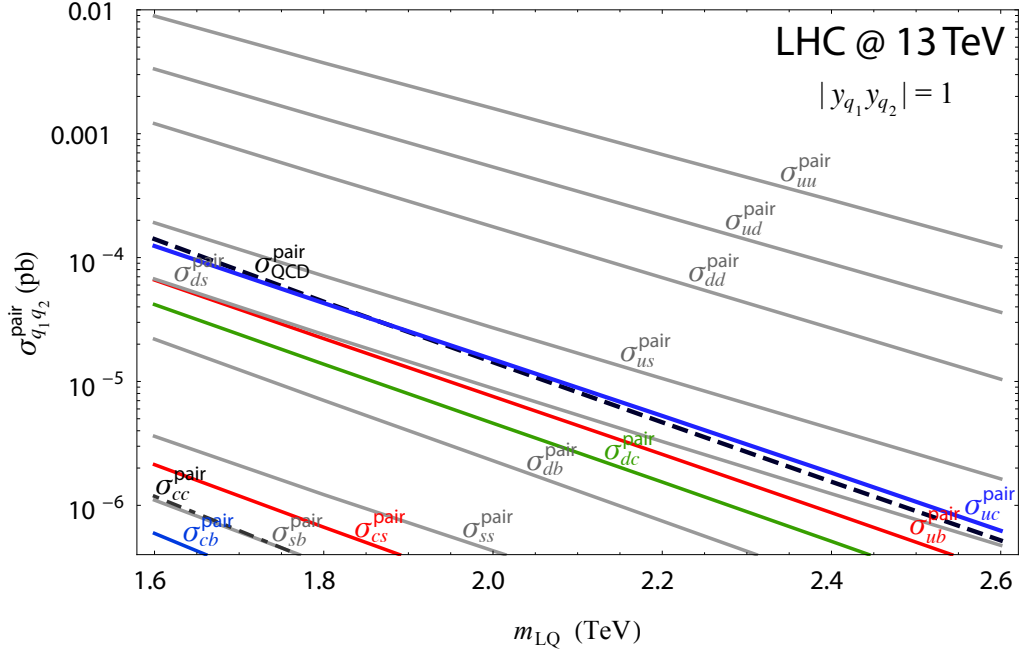


Figure 3. Asymmetric leptoquark pair production cross sections $\sigma_{q_1 q_2}^{\text{pair}}(y_{q_1}, y_{q_2}, m_{LQ})$ for quark-quark initial states, where $q_1 = u, d, s, c$ and $q_2 = u, d, s, c, b$.

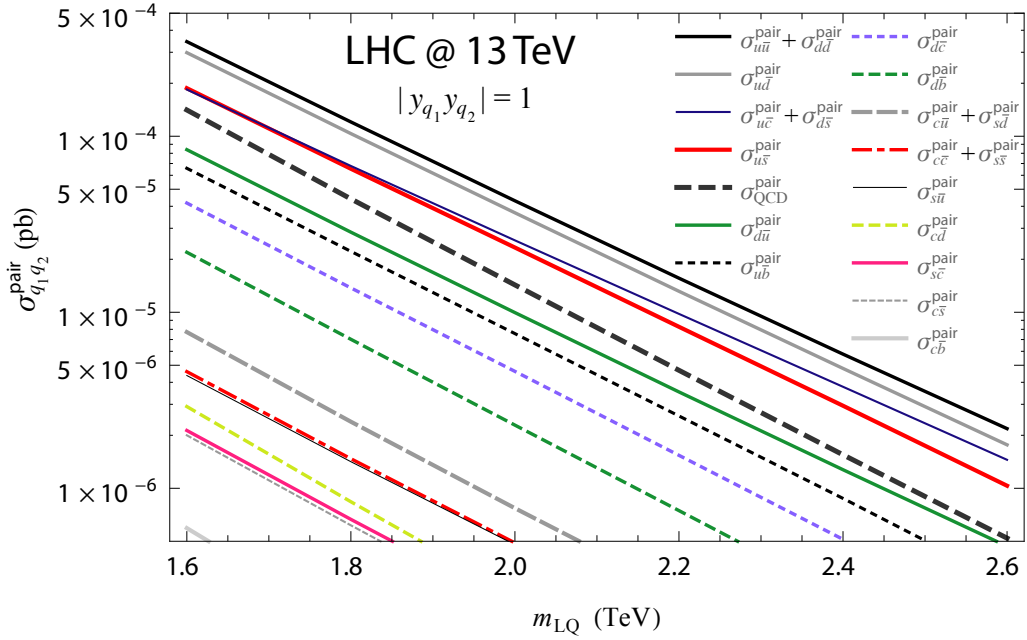


Figure 4. Asymmetric leptoquark pair production cross sections $\sigma_{q_1 q_2}^{\text{pair}}(y_{q_1}, y_{q_2}, m_{LQ})$ for quark-antiquark initial states, where $q_1 = u, d, s, c$ and $q_2 = \bar{u}, \bar{d}, \bar{s}, \bar{c}, \bar{b}$.

the LHC if at least one of the leptoquarks couples to a valence quark and the product of relevant Yukawa couplings is of order one. For example, $\sigma_{uu}^{\text{pair}}(y_{q_1}, y_{q_2}, m_{\text{LQ}})$ for $|y_{q_1} y_{q_2}| = 1$ is approximately two orders of magnitude larger than $\sigma_{\text{QCD}}^{\text{pair}}(m_{\text{LQ}})$. In all other instances, i.e., for $q_1, q_2 = s, c, b$, the cross sections for asymmetric pair production are, at best, a tiny correction of the QCD driven one, again, for order one Yukawa coupling strengths. In the case of the quark-antiquark initiated asymmetric pair production cross sections the only truly relevant scenarios, once again, are those where the initial quark is a valence quark. This is nicely illustrated in Fig. 4 with the direct comparison between the QCD cross section rendered with a black thick dashed curve and the quark-antiquark induced cross sections $\sigma_{q_1 q_2}^{\text{pair}}(y_{q_1}, y_{q_2}, m_{\text{LQ}})$, where $q_1 = u, d, s, c$ and $q_2 = \bar{u}, \bar{d}, \bar{s}, \bar{c}, \bar{b}$ and $|y_{q_1} y_{q_2}| = 1$. The reason why we opted to plot combinations $\sigma_{u\bar{u}}^{\text{pair}} + \sigma_{d\bar{d}}^{\text{pair}}$, $\sigma_{u\bar{c}}^{\text{pair}} + \sigma_{d\bar{s}}^{\text{pair}}$, $\sigma_{c\bar{u}}^{\text{pair}} + \sigma_{s\bar{d}}^{\text{pair}}$ and $\sigma_{c\bar{c}}^{\text{pair}} + \sigma_{s\bar{s}}^{\text{pair}}$ in Fig. 4, instead of individual cross sections, will be elaborated on in Sec. 2.1.5.

Figs. 3 and 4 demonstrate that it is entirely possible to have substantial cross sections for the asymmetric leptoquark pair production even when one of the leptoquarks couples weakly to the first generation of quarks whereas the other leptoquark couples strongly to the second or third generation of quarks as long as they both couple to a lepton of the same flavor and chirality. Of course, quark-quark initiated processes of asymmetric leptoquark pair production, i.e., when $\Delta F = |F(\text{LQ}_1)| - |F(\text{LQ}_2)| = \pm 2$, are potentially much more relevant at the LHC whereas quark-antiquark initiated processes are naturally enhanced at the Tevatron like machines. Note that the QCD cross section drops faster than the asymmetric cross sections as the mass of leptoquarks is increased. This is due to the fact that the gluon-gluon initiated processes start to be subdominant with respect to the processes initiated by quarks once one goes towards the large leptoquark mass limit.

Before we give an explicit example of the potential importance of the asymmetric scalar leptoquark pair production mechanism we want to address one subtlety associated with the conventional leptoquark pair production that has not been discussed in the literature before.

Conventional leptoquark pair production amplitude, when the leptoquarks comprising a pair are charge conjugates of each other, has two distinct contributions at the leading order. The first one is of purely QCD nature whereas the second one exhibits quadratic dependence on the leptoquark Yukawa coupling y_q . For a single scalar leptoquark LQ that couples to a quark q and any lepton l with Yukawa coupling y_q the conventional leptoquark pair production cross section can thus be written as

$$\sigma_{q\bar{q}}^{\text{pair}}(y_q, m_{\text{LQ}}) = \sigma_{\text{QCD}}^{\text{pair}}(m_{\text{LQ}}) + a_{q\bar{q}}^{\text{interference}}(m_{\text{LQ}}) y_q^2 + \sigma_{q\bar{q}}^{\text{pair}}(y_q, y_q, m_{\text{LQ}}), \quad (2.3)$$

where $\sigma_{\text{QCD}}^{\text{pair}}(m_{\text{LQ}})$ and $\sigma_{q\bar{q}}^{\text{pair}}(y_q, y_q, m_{\text{LQ}})$ have been featured before and we assume, for consistency, that y_q is real. If y_q is small, the cross section depends solely on the leptoquark mass m_{LQ} and the particularities associated with the hadron machine itself and it is given by $\sigma_{\text{QCD}}^{\text{pair}}(m_{\text{LQ}})$. In fact, $\sigma_{\text{QCD}}^{\text{pair}}(m_{\text{LQ}})$ has been known analytically at the next-to-leading order in QCD for a long time [7].

The last term in Eq. (2.3) corresponds to a t -channel exchange of a lepton l with the $q\bar{q}$ pair in the initial state. Again, it does not depend on the type of lepton that the

leptoquark couples to and the relevant cross sections are already introduced in Fig. 4 for $y_q = 1$. Finally, there is the interference term $a_{q\bar{q}}^{\text{interference}}(m_{\text{LQ}})y_q^2$ that turns out to always be negative. There is thus a dip in the pair production cross section below the $\sigma_{\text{QCD}}^{\text{pair}}(m_{\text{LQ}})$ value as Yukawa coupling is increased before y_q becomes sufficiently large to make the third term in Eq. (2.3) that is of quartic nature in terms of y_q to start to dominate over the interference term that is of quadratic nature in y_q . We note, that the automated inclusion of the t -channel term at the next-to-leading order in QCD has been recently introduced in the literature [37].

The things, though, can change with regard to interference effect if a scalar leptoquark LQ couples to a quark q and any lepton l with Yukawa coupling y_q and another quark q' and the same lepton with Yukawa coupling $y_{q'}$. There will then exist four interference terms $a_{q\bar{q}}^{\text{interference}}(m_{\text{LQ}})y_q^2$, $a_{q'\bar{q}'}^{\text{interference}}(m_{\text{LQ}})y_{q'}^2$, $a_{q\bar{q}'}^{\text{interference}}(m_{\text{LQ}})y_q y_{q'}$, and $a_{q'\bar{q}}^{\text{interference}}(m_{\text{LQ}})y_q y_{q'}$, where the last two can obviously exhibit constructive interference if y_q and $y_{q'}$ differ in sign. In fact, it might be even possible for both $a_{q\bar{q}}^{\text{interference}}(m_{\text{LQ}})y_q^2$ and $a_{q'\bar{q}'}^{\text{interference}}(m_{\text{LQ}})y_{q'}^2$ to be less relevant than either $a_{q\bar{q}'}^{\text{interference}}(m_{\text{LQ}})y_q y_{q'}$ or $a_{q'\bar{q}}^{\text{interference}}(m_{\text{LQ}})y_q y_{q'}$. The point we want to make here is that the conventional pair production of leptoquarks might be sensitive not only to Yukawa coupling strengths but also to the relative sign between relevant Yukawa couplings even when these couplings are taken to be real.

With these preliminary considerations out of the way we now turn towards quantitative analysis of the asymmetric pair production mechanism within several concrete scenarios of new physics.

2.1 Case studies

Our primary aim is to advocate importance of inclusion of the asymmetric pair production mechanism in a quantitative determination of the viable leptoquark parameter space if and when appropriate. To that end, we discuss five different leptoquark extensions of the SM and derive, for several particular realisations of these extensions, accurate limits using two specific experimental searches. More specifically, we recast the ATLAS Collaboration analysis [1] of the leptoquark pair production searches via $pp \rightarrow \text{LQ}\bar{\text{LQ}} \rightarrow jjee$ and $pp \rightarrow \text{LQ}\bar{\text{LQ}} \rightarrow jj\mu\mu$ processes, where j is taken to generically represent a light jet, i.e., $j = u, \bar{u}, d, \bar{d}, s, \bar{s}$, while it is implicitly understood that both ee and $\mu\mu$ stand for oppositely charged lepton pairs. All five scenarios provide a setting for pedagogical illustration of various phenomenological intricacies associated with the leptoquark pair production signatures.

First of these five scenarios involves a presence of a single scalar leptoquark S_1 . The second scenario of new physics is an R_2 extension of the SM, where R_2 multiplet comprises two states, i.e., $R_2^{+5/3}$ and $R_2^{-2/3}$. Third scenario extends the SM particle content with both S_1 and R_2 while fourth scenario concerns addition of an S_3 leptoquark multiplet to the SM particle content, where S_3 contains scalars $S_3^{+4/3}$, $S_3^{+1/3}$, and $S_3^{-2/3}$. Fifth scenario regards simultaneous extension of the SM with both S_1 and S_3 . We will assume that all these leptoquarks exclusively couple to either electrons or muons and the first generation quarks, to simplify discussion, where, for the electron coupling case, we also produce in

Sec. 3 the latest APV search limits on the leptoquark parameter spaces.

Relevant parts of the S_1 lagrangian, for our study, are

$$\begin{aligned}\mathcal{L}_{S_1} &= + y_{1ij}^{LL} \bar{Q}_L^{C i,a} S_1 \epsilon^{ab} L_L^{j,b} + y_{1ij}^{RR} \bar{u}_R^C S_1 e_R^j + \text{h.c.} \\ &= - (y_1^{LLU})_{ij} \bar{d}_L^C \nu_L^j S_1^{+1/3} + (V^* y_1^{LL})_{ij} \bar{u}_L^C e_L^j S_1^{+1/3} + y_{1ij}^{RR} \bar{u}_R^C e_R^j S_1^{+1/3} + \text{h.c.},\end{aligned}\quad (2.4)$$

where $a, b (= 1, 2)$ are $SU(2)$ indices, V is a Cabibbo–Kobayashi–Maskawa (CKM) mixing matrix, and U represents a Pontecorvo–Maki–Nakagawa–Sakata (PMNS) unitary mixing matrix. We set the CKM matrix to be an identity matrix whereas the exact form of the PMNS matrix is irrelevant for our considerations as long as it resides entirely in the neutrino sector. Note that the CKM matrix, in our convention, is in the up-type quark sector. We will address validity of our assumption that the off-diagonal CKM matrix elements can be neglected and whether the exact placement of the CKM matrix is of any importance.

Pertinent parts of the R_2 lagrangian are

$$\begin{aligned}\mathcal{L}_{R_2} &= - y_{2ij}^{RL} \bar{u}_R^i R_2^a \epsilon^{ab} L_L^{j,b} + y_{2ij}^{LR} \bar{e}_R^i R_2^a Q_L^{j,a} + \text{h.c.} \\ &= - y_{2ij}^{RL} \bar{u}_R^i e_L^j R_2^{+5/3} + (y_2^{RLU})_{ij} \bar{u}_R^i \nu_L^j R_2^{+2/3} + \\ &\quad + (y_2^{LRV^\dagger})_{ij} \bar{e}_R^i u_L^j R_2^{-5/3} + y_{2ij}^{LR} \bar{e}_R^i d_L^j R_2^{-2/3} + \text{h.c.}\end{aligned}\quad (2.5)$$

One can note that all unitary transformations of the right-chiral fermions can be completely absorbed, for both the S_1 and R_2 scenarios, into associated Yukawa coupling matrices. We accordingly take all unitary transformations of right-chiral quarks and charged leptons to be unphysical in our study.

The S_3 Lagrangian, in our notation, is

$$\begin{aligned}\mathcal{L}_{S_3} &= y_{3ij}^{LL} \bar{Q}_L^{C i,a} \epsilon^{ab} (\tau^k S_3^k)^{bc} L_L^{j,c} + \text{h.c.} \\ &= - (y_3^{LLU})_{ij} \bar{d}_L^C \nu_L^j S_3^{+1/3} - (V^* y_3^{LL})_{ij} \bar{u}_L^C e_L^j S_3^{+1/3} + \\ &\quad + \sqrt{2} (V^* y_3^{LLU})_{ij} \bar{u}_L^C \nu_L^j S_3^{-2/3} - \sqrt{2} y_3^{LL} \bar{d}_L^C e_L^j S_3^{+4/3} + \text{h.c.},\end{aligned}\quad (2.6)$$

where τ^k , $k = 1, 2, 3$, are Pauli matrices and we define $S_3^{+4/3} = (S_3^1 - iS_3^2)/\sqrt{2}$, $S_3^{+1/3} = S_3^3$, and $S_3^{-2/3} = (S_3^1 + iS_3^2)/\sqrt{2}$ to be electric charge eigenstates.

Again, in all of these scenarios we will always assume a presence of a single non-zero Yukawa coupling to either electron or muon and the first generation quarks for each of these leptoquark multiplets, if and when they are featured, in order to simplify discussion.

2.1.1 Case study: $S_1(\bar{\mathbf{3}}, \mathbf{1}, 1/3)$

Let us first address the S_1 scenario.

- If we assume that $y_{111}^{LL} \equiv y$ is the only non-zero Yukawa coupling present in Eq. (2.4), we have that the branching ratios for the S_1 decays are $B(S_1^{\pm 1/3} \rightarrow j\nu) = 1/2$ and $B(S_1^{\pm 1/3} \rightarrow je) = 1/2$. A recast of the ATLAS Collaboration analysis [1] of the leptoquark pair production search via $pp \rightarrow \text{LQL}\bar{Q} \rightarrow jjee$ process at 13 TeV center-of-mass energy of proton-proton collisions, using an integrated luminosity of 139 fb^{-1} ,

then yields a limit on the mass of S_1 leptoquark, as a function of $y \equiv y_{11}^{LL}$, which is rendered with a thick dashed black curve in Fig. 5. The exclusion region is to the left of that curve and it is based on the ATLAS Collaboration observed 95% C.L. limit. The Yukawa dependent limit we present in Fig. 5, for small values of $y_{11}^{LL} \equiv y$, needs to agree with the outcome of the ATLAS Collaboration analysis when $B(S_1^{\pm 1/3} \rightarrow je) = 1/2$, i.e. $m_{LQ} \geq 1380$ GeV, which is based on the next-to-leading order cross section in QCD calculation [1]. We accordingly rescale our leading order simulation when presenting the limits in Fig. 5 and note that the cross section obtained in that way indeed corresponds to the next-to-leading order cross section in QCD as given in Ref. [9]. We also plot in Fig. 5 the leptoquark parameter constraint with a vertical thin dashed black line if one would use $\sigma_{\text{QCD}}^{\text{pair}}(m_{LQ})$ instead of the Yukawa dependant cross section, for this particular branching fraction scenario. That vertical line is additionally marked with “w/o t -channels” to stress exclusion of the t -channel lepton exchange diagrams during evaluation of $\sigma_{\text{QCD}}^{\text{pair}}(m_{LQ})$.

We note two subtleties with regard to the $y_{11}^{LL} \equiv y \neq 0$ case. First, there are two t -channel contributions towards the S_1 pair production that need to be included in this analysis. One contribution is due to the first term in the second line of Eq. (2.4) and it is $d\bar{d}$ initiated. The other contribution is $u\bar{u}$ initiated and it is due to the second term in the second line of Eq. (2.4). Another subtlety concerns the CKM mixing matrix placement. Namely, if the CKM matrix is taken to be in the up-type quark sector it would induce coupling between S_1 , a charm quark, and an electron through the second term in the second line of Eq. (2.4). This would primarily impact the branching ratio $B(S_1^{\pm 1/3} \rightarrow je)$ by reducing it to 80% of its initial value and would also introduce $B(S_1^{\pm 1/3} \rightarrow ce)$ at the level of 10%. These changes in branching fractions would consequentially impact interpretation of the ATLAS Collaboration analysis [1] that can distinguish between light jets and, for example, a c -quark induced jet. The bounds on the S_1 parameter space would accordingly shift to the left in Fig. 5. The placement of the CKM mixing matrix in the down-type quark sector, on the other hand, would not produce any such shift.

- If we take $y_{12}^{LL} \equiv y \neq 0$ in Eq. (2.4), the branching ratios for the S_1 decays read $B(S_1^{\pm 1/3} \rightarrow j\nu) = 1/2$ and $B(S_1^{\pm 1/3} \rightarrow j\mu) = 1/2$. A recast of the ATLAS Collaboration analysis [1] of the leptoquark pair production search via $pp \rightarrow LQ\bar{L}\bar{Q} \rightarrow jj\mu\mu$ process then yields a limit on the mass of S_1 leptoquark, as a function of $y \equiv y_{12}^{LL}$, which is rendered with a thick dashed black curve in Fig. 6. The limit we present in Fig. 6, for small values of $y_{12}^{LL} \equiv y$, corresponds to the outcome of the ATLAS Collaboration analysis when $B(S_1^{\pm 1/3} \rightarrow j\mu) = 1/2$, i.e. $m_{LQ} \geq 1420$ GeV, that is shown as a vertical thin dashed black line in Fig. 6.
- If we take that $y_{11}^{RR} \equiv y$ is the only non-zero Yukawa coupling in Eq. (2.4), we get that $B(S_1^{\pm 1/3} \rightarrow je) = 1$ and the correct interpretation of the ATLAS Collaboration results [1] would correspond to a bound rendered with a thick dashed blue curve in Fig. 5. This bound, for small values of $y_{11}^{RR} \equiv y$, yields $m_{LQ} \geq 1790$ GeV [1]

and thus coincides with the constraint presented with a vertical thin dashed blue line that is generated if one were to use $\sigma_{\text{QCD}}^{\text{pair}}(m_{\text{LQ}})$ instead of the more appropriate $\sigma_{u\bar{u}}^{\text{pair}}(y, m_{\text{LQ}})$ to interpret the ATLAS Collaboration analysis.

- If we take that $y_{112}^{RR} \equiv y \neq 0$, a recast of the ATLAS Collaboration results [1] on the $pp \rightarrow \text{LQ}\overline{\text{LQ}} \rightarrow jj\mu\mu$ process search yields a bound rendered with a thick dashed blue curve in Fig. 6. This bound, for small values of $y_{112}^{RR} \equiv y$, reads $m_{\text{LQ}} \geq 1730 \text{ GeV}$ [1] and is given with a vertical thin dashed blue line in Fig. 6.

Note that the exclusion regions, in all four cases, feature negative interference effects, as discussed in connection to Eq. (2.3), for intermediate values of Yukawa couplings $y_{111}^{LL} \equiv y$, $y_{112}^{LL} \equiv y$, $y_{111}^{RR} \equiv y$, and $y_{112}^{RR} \equiv y$.

2.1.2 Case study: $R_2(3, 2, 7/6)$

We consider, in what follows, scenarios when we switch on, individually, y_{211}^{RL} , y_{212}^{RL} , y_{211}^{LR} , and y_{212}^{LR} of Eq. (2.5) while all other Yukawa matrix elements are taken to be negligible.

- If we turn on Yukawa coupling $y_{211}^{RL} \equiv y$ in Eq. (2.5), we have that $B(R_2^{\pm 5/3} \rightarrow je) = 1$ and $B(R_2^{\pm 2/3} \rightarrow j\nu) = 1$. Since the members of the R_2 multiplet need to be mass-degenerate for all practical purposes, the limit on the $R_2^{\pm 5/3}$ parameter space, as extracted from the ATLAS Collaboration pair production analysis [1], should also be applicable to $R_2^{\pm 2/3}$ and vice versa. If we furthermore take into account the fact that the experimental limit on $pp \rightarrow R_2^{+5/3} R_2^{-5/3} \rightarrow jjee$ is certainly more relevant than the limit that could be extracted from $pp \rightarrow R_2^{+2/3} R_2^{-2/3} \rightarrow jj\nu\nu$, the constraint on the viable $R_2^{\pm 5/3}$ and $R_2^{\pm 2/3}$ parameter spaces is given with a thick dashed blue curve in Fig. 5. Note that this particular limit on the $R_2^{\pm 5/3}$ and $R_2^{\pm 2/3}$ parameter spaces, when $y_{211}^{RL} \equiv y \neq 0$, is the same as for S_1 leptoquark when $y_{111}^{RR} \equiv y \neq 0$.
- If we assume that $y_{212}^{RL} \equiv y \neq 0$ in Eq. (2.5), we have that $B(R_2^{\pm 5/3} \rightarrow j\mu) = 1$ and $B(R_2^{\pm 2/3} \rightarrow j\nu) = 1$. In analogy to the previous case the reinterpretation of the ATLAS Collaboration pair production analysis [1] of the $pp \rightarrow \text{LQ}\overline{\text{LQ}} \rightarrow jj\mu\mu$ process search yields a constraint on the viable $R_2^{\pm 5/3}$ and $R_2^{\pm 2/3}$ parameter spaces that is given with a thick dashed blue curve in Fig. 6. A vertical thin dashed blue line in Fig. 6 represents a limit that is based solely on the QCD cross section and corresponds to $m_{\text{LQ}} \geq 1730 \text{ GeV}$ [1]. The limits on the $R_2^{\pm 5/3}$ and $R_2^{\pm 2/3}$ parameter spaces, when $y_{212}^{RL} \equiv y \neq 0$, are the same as for S_1 leptoquark when $y_{112}^{RR} \equiv y \neq 0$.
- If we set $y_{211}^{LR} \equiv y \neq 0$, we have that $B(R_2^{\pm 5/3} \rightarrow je) = 1$ and $B(R_2^{\pm 2/3} \rightarrow je) = 1$. Since the pair productions of both components of R_2 produce the same final state, i.e., $pp \rightarrow R_2^{+5/3} R_2^{-5/3} \rightarrow jjee$ and $pp \rightarrow R_2^{+2/3} R_2^{-2/3} \rightarrow jjee$, we need to take that into account. Naive combination of these two processes, i.e., based purely on the $\sigma_{\text{QCD}}^{\text{pair}}(m_{\text{LQ}})$ value, results in a bound given by a vertical thin dashed red line in Fig. 5 and yields $m_{\text{LQ}} \geq 1920 \text{ GeV}$. If we furthermore include the Yukawa dependence of the cross sections to pair produce both components of R_2 multiplet, we obtain a

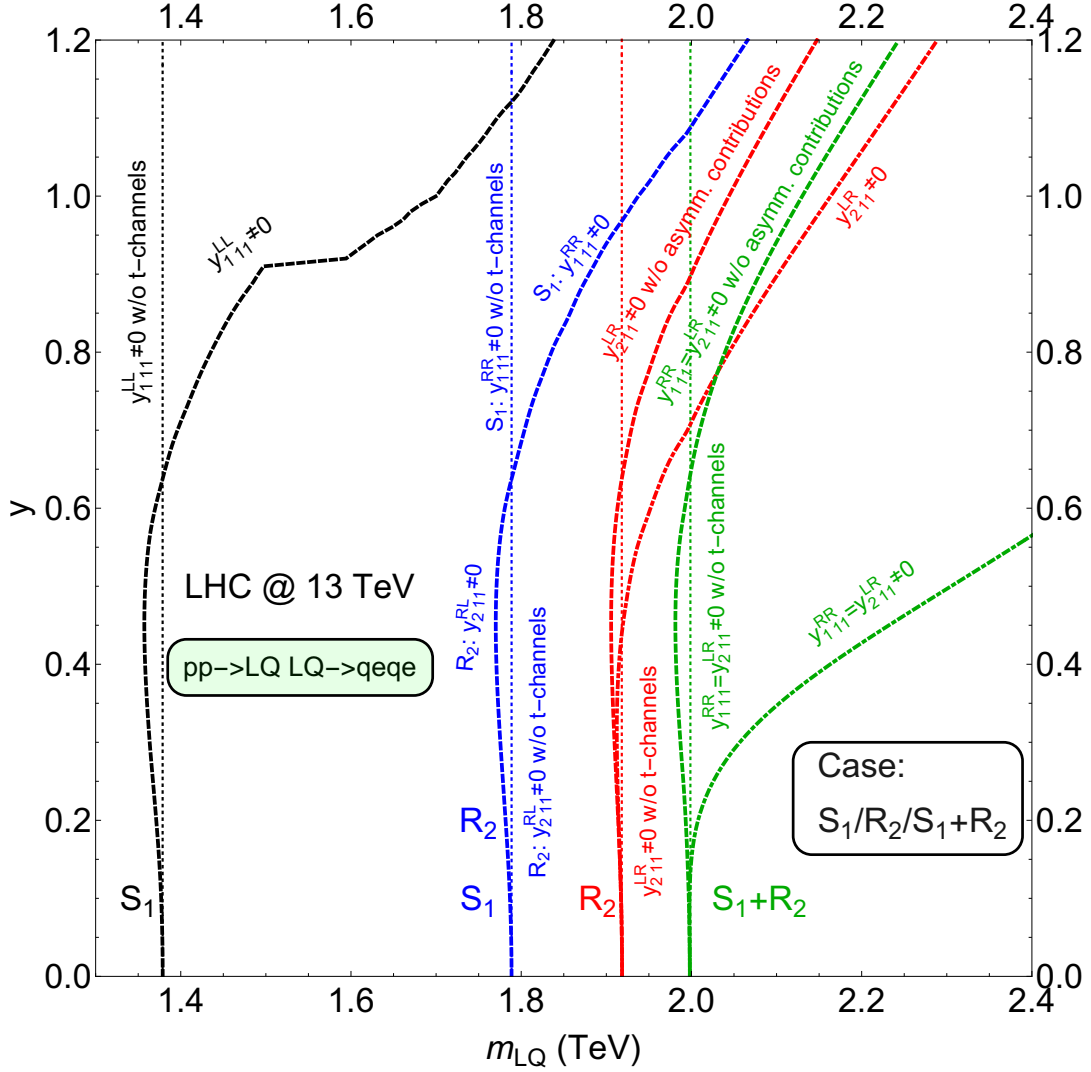


Figure 5. The leptoquark parameter space limits for the S_1 , R_2 , and S_1+R_2 scenarios extracted from the $pp \rightarrow LQ\bar{L}\bar{Q} \rightarrow jjee$ process search [1] performed at 13 TeV center-of-mass energy of proton-proton collisions at the LHC, using an integrated luminosity of 139 fb^{-1} . See text for more details.

limit rendered in a thick dashed red curve in Fig. 5. It should be noted that the generation of the thick dashed red curve denoted with “w/o asymm. contributions” calls for separate evaluation of cross sections for both $pp \rightarrow R_2^{+5/3} R_2^{-5/3} (\rightarrow jjee)$ and $pp \rightarrow R_2^{+2/3} R_2^{-2/3} (\rightarrow jjee)$ and their subsequent addition. Since $R_2^{-5/3}$ couples to the up quark while $R_2^{-2/3}$ couples to the down quark, these two cross sections, as functions of $y_{21}^{LR} \equiv y$, are clearly not identical.

Note, however, that simple addition of cross sections to produce $R_2^{+5/3} R_2^{-5/3}$ and $R_2^{+2/3} R_2^{-2/3}$ pairs does not account for the asymmetric pair production mechanism effects that we want to advocate. To take into account asymmetric pair production we also need to include cross sections for $pp \rightarrow R_2^{+5/3} R_2^{-2/3} (\rightarrow jjee)$ and $pp \rightarrow$

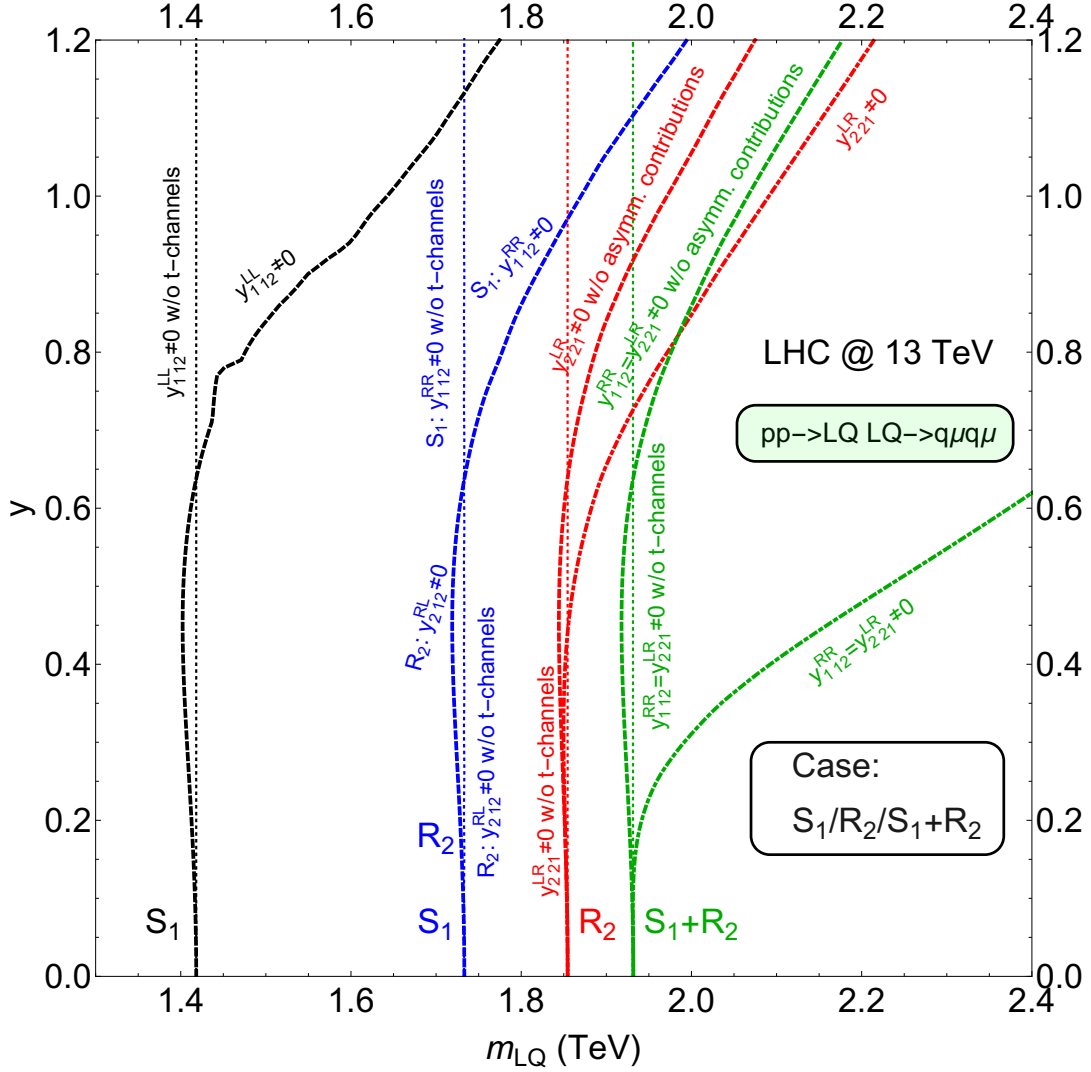


Figure 6. The leptoquark parameter space limits for the S_1 , R_2 , and S_1+R_2 scenarios extracted from the $pp \rightarrow LQ\bar{L}Q \rightarrow jj\mu\mu$ process search [1] performed at 13 TeV center-of-mass energy of proton-proton collisions at the LHC, using an integrated luminosity of 139 fb^{-1} . See text for more details.

$R_2^{-5/3}R_2^{+2/3}(\rightarrow jjee)$. Relevant diagrams for these two processes are presented in Fig. 7. The diagrams of Fig. 7 explicitly show that the two leptoquarks that are produced do not comprise a charge conjugate pair. These processes thus do not interfere, at the amplitude level, with the conventional pair production mechanisms even though they yield the exact same $jjee$ final state.

If we combine both the conventional and asymmetric pair production cross sections, and apply the constraints obtained by the ATLAS Collaboration on the $pp \rightarrow LQ\bar{L}Q \rightarrow jjee$ process [1], we obtain a proper bound rendered with a thick dot-dashed red curve in Fig. 5. The relevance of the asymmetric contribution is, in our view, self-evident.

We finally present, for completeness, the leading order cross sections for $pp \rightarrow R_2^{+5/3} R_2^{-5/3}$, $pp \rightarrow R_2^{+2/3} R_2^{-2/3}$, $pp \rightarrow R_2^{+5/3} R_2^{-2/3}$, and $pp \rightarrow R_2^{-5/3} R_2^{+2/3}$ in Table 4 as functions of $y \equiv y_{211}^{LR}$ and m_{LQ} . Note, again, that the cross sections for $pp \rightarrow R_2^{+5/3} R_2^{-5/3}$ and $pp \rightarrow R_2^{+2/3} R_2^{-2/3}$ behave differently with respect to change of $y_{211}^{LR} \equiv y$.

- If we set $y_{212}^{LR} \equiv y \neq 0$, we have that $B(R_2^{\pm 5/3} \rightarrow j\mu) = 1$ and $B(R_2^{\pm 2/3} \rightarrow j\mu) = 1$. The limits presented in Fig. 6 in red with a vertical thin dashed line, a thick dashed curve, and a thick dot-dashed curve correspond to a QCD only limit, a conventional Yukawa coupling dependent limit, and a proper limit that includes asymmetric production effects, respectively. These limits converge to the same bound of $m_{LQ} \geq 1850$ GeV, as required by the observed 95% C.L. limit of the ATLAS Collaboration search for the $pp \rightarrow LQ\bar{L}\bar{Q} \rightarrow jj\mu\mu$ process [1].

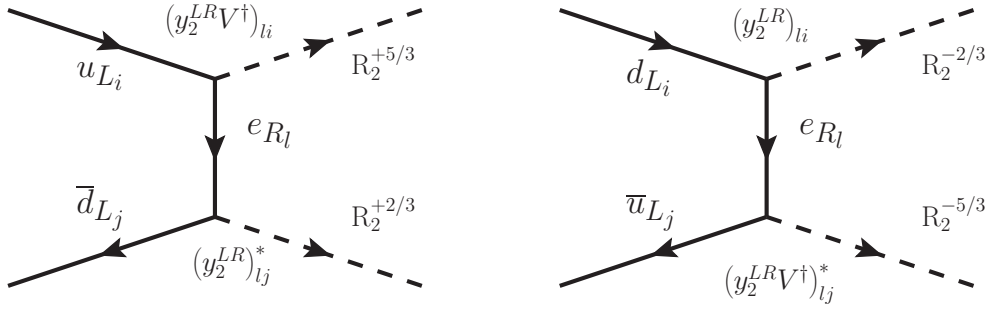


Figure 7. Asymmetric pair production for the case of R_2 leptoquark.

2.1.3 Case study: $S_1(\bar{\mathbf{3}}, \mathbf{1}, 1/3) + R_2(\mathbf{3}, \mathbf{2}, 7/6)$

Since both S_1 and R_2 multiplets can couple to the SM leptons of both chiralities, there are four different scenarios to consider even if only one Yukawa coupling for each of these two multiplets is turned on at a given time. To avoid overburdening the reader with too many details and to drive our point of potential importance of the asymmetric pair production inclusion, we will investigate only one of these four possibilities for both the $jjee$ and $jj\mu\mu$ final state scenarios.

- We first take that $y_{111}^{RR} = y_{211}^{LR} \equiv y \neq 0$ so that all three leptoquarks decay into the same final state, i.e., $B(S_1^{\pm 1/3} \rightarrow je) = B(R_2^{\pm 5/3} \rightarrow je) = B(R_2^{\pm 2/3} \rightarrow je) = 1$. If we furthermore take that the masses of S_1 and of the two charged components in R_2 are the same, we obtain that a pure QCD cross section generates bound given with a vertical thin dashed green line whereas a simplistic addition of cross

m_{LQ}	y	$\sigma_{R_2^{+2/3}R_2^{-2/3}}$ (fb)	$\sigma_{R_2^{+5/3}R_2^{-5/3}}$ (fb)	$\sigma_{R_2^{+5/3}R_2^{-2/3}}$ (fb)	$\sigma_{R_2^{-5/3}R_2^{+2/3}}$ (fb)
1.6 TeV	0.1	0.141	0.141	2.98×10^{-5}	8.39×10^{-6}
	0.5	0.138	0.132	0.0187	0.00523
	1.0	0.201	0.287	0.298	0.0837
2.0 TeV	0.1	0.0143	0.0143	3.67×10^{-6}	9.93×10^{-7}
	0.5	0.0139	0.0131	0.00292	0.000622
	1.0	0.0210	0.0331	0.0367	0.00996
2.4 TeV	0.1	0.00157	0.00156	4.80×10^{-7}	1.28×10^{-7}
	0.5	0.00151	0.00139	2.99×10^{-4}	0.796×10^{-4}
	1.0	0.00239	0.00414	0.00482	0.00128

Table 4. The leading order cross sections for the leptoquark pair production for the R_2 scenario in the proton-proton collisions at 13 TeV center-of-mass energy when the R_2 components of mass m_{LQ} couple exclusively to a right-chiral leptons and the first generation quarks, as allowed by the SM gauge group, with the coupling strength $y \equiv y_2^{LR}$.

sections for processes $pp \rightarrow S_1^{+1/3}S_1^{-1/3}(\rightarrow jjee)$, $pp \rightarrow R_2^{+5/3}R_2^{-5/3}(\rightarrow jjee)$, and $pp \rightarrow R_2^{+2/3}R_2^{-2/3}(\rightarrow jjee)$ yields a bound given by a thick dashed green curve in Fig. 5. These bounds are based on the observed 95% C.L. limits, as given by the ATLAS Collaboration results on the $pp \rightarrow \text{LQL}\bar{\text{Q}} \rightarrow jjee$ process search [1], and yield $m_{\text{LQ}} \geq 2000$ GeV in the small Yukawa coupling limit. Since the ATLAS Collaboration analysis [1] provides results for the leptoquark masses up to 2 TeV only, we conservatively assume that the observed limits above 2 TeV would have the ATLAS Collaboration 2 TeV level values.

If we finally include all six asymmetric contributions, i.e., $pp \rightarrow S_1^{\pm 1/3}R_2^{\pm 5/3}(\rightarrow jjee)$, $pp \rightarrow S_1^{\pm 1/3}R_2^{\pm 2/3}(\rightarrow jjee)$, and $pp \rightarrow R_2^{\pm 5/3}R_2^{\mp 2/3}(\rightarrow jjee)$, we obtain a bound given by a thick dot-dashed green curve in Fig. 5. Once again, the importance of inclusion of the asymmetric contribution is, in our view, self-evident.

- If we take that $y_{112}^{RR} = y_{212}^{LR} \equiv y \neq 0$ so that all three leptoquarks decay into muons and light jets, i.e., $B(S_1^{\pm 1/3} \rightarrow j\mu) = B(R_2^{\pm 5/3} \rightarrow j\mu) = B(R_2^{\pm 2/3} \rightarrow j\mu) = 1$, we obtain the limits rendered in Fig. 6 in green. These limits are obtained under the assumption that all three leptoquarks are mass-degenerate and represent a recast of the ATLAS Collaboration search for the $pp \rightarrow \text{LQL}\bar{\text{Q}} \rightarrow jj\mu\mu$ process [1]. A vertical thin dashed line is generated by a pure QCD cross section, a thick dashed curve is produced by a simple inclusion of the Yukawa dependent terms in the relevant cross sections while a thick dot-dashed curve corresponds to the correct inclusion of both the conventional and asymmetric contributions towards total cross section that yields the $jj\mu\mu$ final state. These three limits, rendered in green in Fig. 6, converge to $m_{\text{LQ}} \geq 1930$ GeV for small values of $y_{112}^{RR} = y_{212}^{LR} \equiv y$.

2.1.4 Case study: $S_3(\bar{\mathbf{3}}, \mathbf{3}, 1/3)$

We consider two particular scenarios for the S_3 case. One scenario is when $y_{311}^{LL} \neq 0$ and the other one is when $y_{312}^{LL} \neq 0$.

- We assume that $y_{311}^{LL} \equiv y$ of Eq. (2.6) is the only non-zero Yukawa coupling and take all three leptoquarks within S_3 multiplet to be degenerate in mass that we denote by m_{LQ} . The branching fractions for the S_3 components, when $y_{311}^{LL} \neq 0$, are $B(S_3^{\pm 4/3} \rightarrow j\bar{j}e) = 1$, $B(S_3^{\pm 2/3} \rightarrow j\nu) = 1$, $B(S_3^{\pm 1/3} \rightarrow j\bar{j}e) = 1/2$, and $B(S_3^{\pm 1/3} \rightarrow j\nu) = 1/2$.

If we are to use the ATLAS Collaboration results on the $pp \rightarrow LQ\bar{LQ} \rightarrow j\bar{j}e\bar{e}$ process [1] to generate accurate constraints on the S_3 parameter space, we need to take into account several factors. Namely, in the regime of the QCD dominated leptoquark pair production, i.e., for small y_{311}^{LL} , there are two different processes that yield the $j\bar{j}e\bar{e}$ final state. These are $pp \rightarrow S_3^{+4/3}S_3^{-4/3} \rightarrow j\bar{j}e\bar{e}$ and $pp \rightarrow S_3^{+1/3}S_3^{-1/3} \rightarrow j\bar{j}e\bar{e}$, where the $S_3^{+4/3}S_3^{-4/3}$ pair goes exclusively into $j\bar{j}e\bar{e}$ whereas the $S_3^{+1/3}S_3^{-1/3}$ pair decays into $j\bar{j}e\bar{e}$ only 25% of the time. If y_{311}^{LL} is not small, we need to include conventional t -channel contributions that were discussed in the context of Eq. (2.3). These contributions, however, are not the same for $pp \rightarrow S_3^{+4/3}S_3^{-4/3}$ and $pp \rightarrow S_3^{+1/3}S_3^{-1/3}$ since the former process is $\bar{d}\bar{d}$ initiated whereas the latter one is both $u\bar{u}$ and $\bar{d}\bar{d}$ initiated. Moreover, the $S_3^{\pm 4/3}$ couplings to the quark-lepton pairs are always a factor of $\sqrt{2}$ larger than that of $S_3^{\pm 1/3}$ due to the $SU(2)$ symmetry of the SM. If we account for all these intricacies, we obtain the Yukawa dependent limit given in Fig. 9 with a thick dashed red curve. A vertical thin dashed red line in Fig. 9, on the other hand, denotes a naive limit if we were to use purely QCD dominated leptoquark pair production cross sections and yields $m_{LQ} \geq 1830$ GeV. We opted not to present the S_3 results with all other scenarios discussed previously in Fig. 5 in order to provide ease of readability. Note, however, that we provide in Fig. 9 limits on the S_1 scenarios that were already discussed in Sec. 2.1.1 and also presented in Fig. 5 for comparison purposes.

Our considerations, up to this point, did not incorporate potential asymmetric production contributions towards the $j\bar{j}e\bar{e}$ final state. There are, in general, four asymmetric pair production contributions in any S_3 scenario and we present associated diagrams in Fig. 8. Two diagrams in the second row of Fig. 8 can give the $j\bar{j}e\bar{e}$ final state via $pp \rightarrow S_3^{-4/3}S_3^{+1/3} \rightarrow j\bar{j}e\bar{e}$ and $pp \rightarrow S_3^{+4/3}S_3^{-1/3} \rightarrow j\bar{j}e\bar{e}$ with 50% probability, each, where $pp \rightarrow S_3^{-4/3}S_3^{+1/3}$ and $pp \rightarrow S_3^{+4/3}S_3^{-1/3}$ are $u\bar{d}$ and $\bar{d}u$ initiated, respectively. If we account for these effects, we obtain a limit given in Fig. 9 with a thick dot-dashed red curve. It is this limit that represents correct interpretation of the ATLAS Collaboration results on the $pp \rightarrow LQ\bar{LQ} \rightarrow j\bar{j}e\bar{e}$ process [1] when $y_{311}^{LL} \equiv y$ of Eq. (2.6) is the only non-zero Yukawa coupling. Again, the importance of the asymmetric production inclusion is self-evident.

- We assume that $y_{312}^{LL} \equiv y$ of Eq. (2.6) is the only non-zero Yukawa coupling and take all three leptoquarks within S_3 multiplet to be degenerate. The branching fractions for the S_3 components, when $y_{312}^{LL} \neq 0$, are $B(S_3^{\pm 4/3} \rightarrow j\mu) = 1$, $B(S_3^{\pm 2/3} \rightarrow j\nu) = 1$,

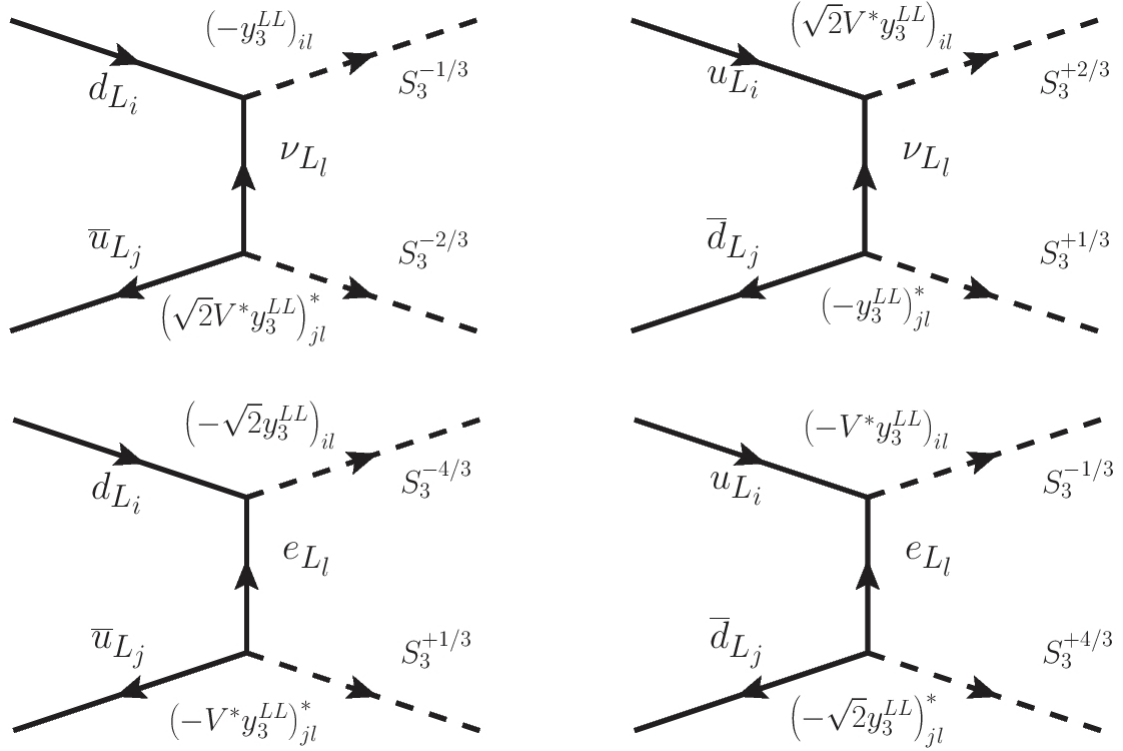


Figure 8. Asymmetric pair production for the case of S_3 leptoquark.

$B(S_3^{\pm 1/3} \rightarrow j\mu) = 1/2$, and $B(S_3^{\pm 1/3} \rightarrow j\nu) = 1/2$. Following the procedure already outlined for the recast of the $y_{311}^{LL} \equiv y \neq 0$ case and applying it on the results of the ATLAS Collaboration search for the $pp \rightarrow LQ\bar{L}\bar{Q} \rightarrow jj\mu\mu$ process [1], we obtain limits rendered in red in Fig. 10. These converge at $m_{LQ} \geq 1770$ GeV for small values of $y_{312}^{LL} \equiv y$.

2.1.5 Case study: $S_1(\bar{\mathbf{3}}, \mathbf{1}, 1/3) + S_3(\bar{\mathbf{3}}, \mathbf{3}, 1/3)$

Since S_3 couples exclusively to the left-chiral leptons we will assume that the only non-zero Yukawa couplings in this scenario, comprising S_1 and S_3 leptoquarks, are either y_{111}^{LL} and y_{311}^{LL} or y_{112}^{LL} and y_{312}^{LL} . This ansatz will allow us to present an analysis of the asymmetric pair production effects within the $\Delta F = 0$ system.

- We first consider scenario with $y_{111}^{LL} \neq 0$ and $y_{311}^{LL} \neq 0$. The branching fractions of leptoquarks are $B(S_3^{\pm 4/3} \rightarrow je) = 1$, $B(S_3^{\pm 2/3} \rightarrow j\nu) = 1$, $B(S_3^{\pm 1/3} \rightarrow je) = 1/2$, $B(S_3^{\pm 1/3} \rightarrow j\nu) = 1/2$, $B(S_1^{\pm 1/3} \rightarrow je) = 1/2$, and $B(S_1^{\pm 1/3} \rightarrow j\nu) = 1/2$. We furthermore assume that S_1 and the components of S_3 are degenerate in mass and also take that $y_{111}^{LL} = y_{311}^{LL} \equiv y$ to simplify discussion.

A naive QCD limit on the parameter space of this scenario, set by the ATLAS Collaboration data on the $pp \rightarrow LQ\bar{L}\bar{Q} \rightarrow jjee$ process [1], is presented in Fig. 9

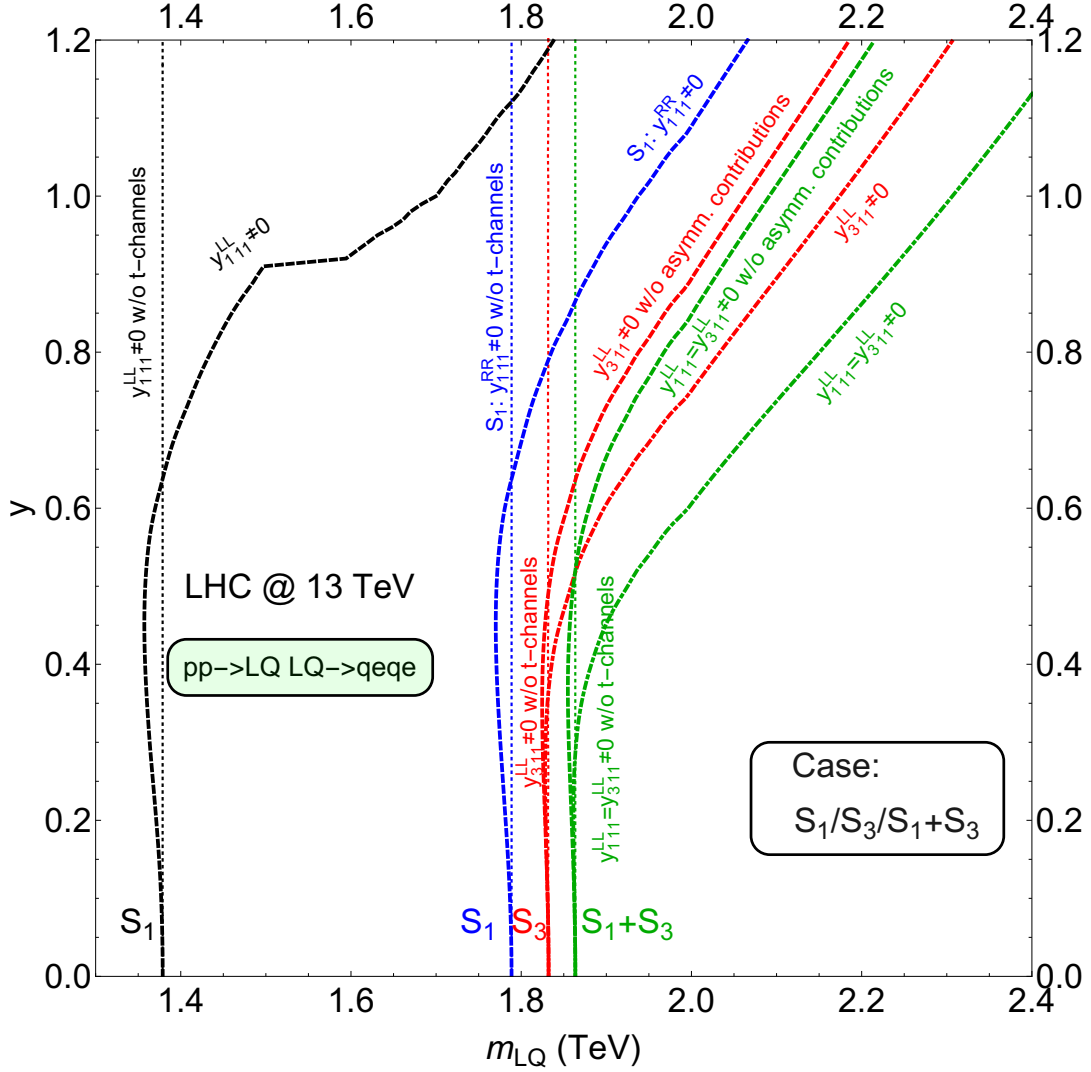


Figure 9. The leptoquark parameter space limits for the S_1 , S_3 , and S_1+S_3 scenarios extracted from the $pp \rightarrow LQ\bar{L}Q \rightarrow jjee$ process search [1] performed at 13 TeV center-of-mass energy of proton-proton collisions at the LHC, using an integrated luminosity of 139 fb^{-1} . See text for more details.

with a vertical thin dashed green line and corresponds to $m_{LQ} \geq 1860 \text{ GeV}$. If we also include the usual t -channel contributions for both S_1 and S_3 , as discussed previously in Secs. 2.1.1 and 2.1.4, respectively, we obtain the limit given with a thick dashed green curve in Fig. 9.

In order to numerically evaluate the asymmetric pair production contributions we need to account for $pp \rightarrow S_3^{-4/3} S_3^{+1/3} \rightarrow jjee$ (50%), $pp \rightarrow S_3^{+4/3} S_3^{-1/3} \rightarrow jjee$ (50%), $pp \rightarrow S_3^{-4/3} S_1^{+1/3} \rightarrow jjee$ (50%), $pp \rightarrow S_3^{+4/3} S_1^{-1/3} \rightarrow jjee$ (50%), $pp \rightarrow S_3^{-1/3} S_1^{+1/3} \rightarrow jjee$ (25%) and $pp \rightarrow S_3^{+1/3} S_1^{-1/3} \rightarrow jjee$ (25%), where we specify in parentheses the associated decay rate into the $jjee$ final state for each of these processes. Note that the last two processes are both $u\bar{u}$ and $d\bar{d}$ initiated. In fact,

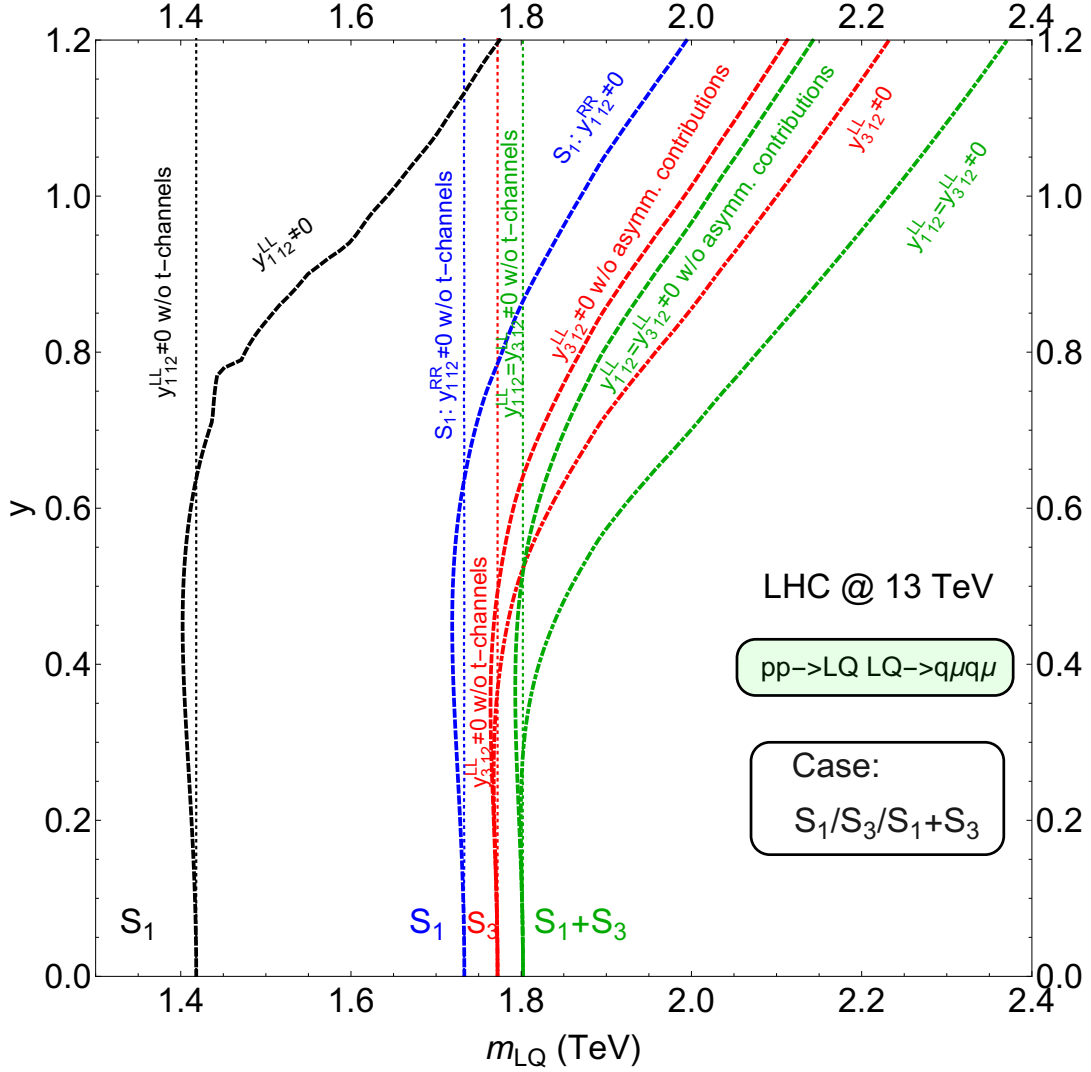


Figure 10. The leptoquark parameter space limits for the S_1 , S_3 , and S_1+S_3 scenarios extracted from the $pp \rightarrow LQ\bar{L}Q \rightarrow jj\mu\mu$ process search [1] performed at 13 TeV center-of-mass energy of proton-proton collisions at the LHC, using an integrated luminosity of 139 fb^{-1} . See text for more details.

S_1+S_3 scenario is the only $\Delta F = 0$ scenario that features asymmetric production initiated with the $q\bar{q}'$ combination, where both q and q' are of the same type of flavor. Moreover, these same-flavor contributions always come in pairs as they are simultaneously generated by the up-type and down-type quarks. This is the reason why we opted to present combinations $\sigma_{u\bar{u}}^{\text{pair}} + \sigma_{d\bar{d}}^{\text{pair}}$, $\sigma_{u\bar{c}}^{\text{pair}} + \sigma_{d\bar{s}}^{\text{pair}}$, $\sigma_{c\bar{u}}^{\text{pair}} + \sigma_{s\bar{d}}^{\text{pair}}$ and $\sigma_{c\bar{c}}^{\text{pair}} + \sigma_{s\bar{s}}^{\text{pair}}$ in Fig. 4 instead of individual $q\bar{q}'$ contributions.

If we properly include all the relevant processes that yield the $jj\mu\mu$ final state, we obtain a limit on the S_1+S_3 scenario parameter space that is given by a thick dot-dashed green curve in Fig. 9. The parameter space to the left of that curve is excluded by the ATLAS Collaboration search for the $pp \rightarrow LQ\bar{L}Q \rightarrow jj\mu\mu$ process [1].

- If we assume that $y_{12}^{LL} \neq 0$ and $y_{32}^{LL} \neq 0$, the branching fractions of leptoquarks read $B(S_3^{\pm 4/3} \rightarrow j\mu) = 1$, $B(S_3^{\pm 2/3} \rightarrow j\nu) = 1$, $B(S_3^{\pm 1/3} \rightarrow j\mu) = 1/2$, $B(S_3^{\pm 1/3} \rightarrow j\nu) = 1/2$, $B(S_1^{\pm 1/3} \rightarrow j\mu) = 1/2$, and $B(S_1^{\pm 1/3} \rightarrow j\nu) = 1/2$. If we also assume that S_1 and the components of S_3 are degenerate in mass and take that $y_{12}^{LL} = y_{32}^{LL} \equiv y$, we obtain the set of limits rendered in green in Fig. 10 that converge to $m_{LQ} \geq 1800$ GeV for small values of $y_{12}^{LL} = y_{32}^{LL} \equiv y$. These limits use the ATLAS Collaboration search results for the $pp \rightarrow LQ\bar{L}\bar{Q} \rightarrow jj\mu\mu$ process [1]. A vertical thin dashed line is the bound based on the QCD cross section. A thick dashed curve is generated if one accounts for the usual t -channel contributions whereas a thick dot-dashed curve is the accurate limit that incorporates both the conventional and asymmetric leptoquark pair production mechanism effects.

2.2 Final remarks

Before we conclude this section, several remarks are in order.

- We have explicitly assumed in our analysis that the asymmetrically produced leptoquarks are mass degenerate. If that is not the case the asymmetric pair production mechanism would allow for an unambiguous and unique test of existence of multiple leptoquarks if the leptoquarks in question couple to the lepton(s) of the same chirality. The asymmetric pair production search would thus be complementary to other detection methods, either direct or indirect, to ascertain the existence of these hypothetical particles at hadron colliders.
- We have not included the CKM matrix effects in our numerical study. We have, however, commented in Sec. 2.1.1 on the fact that the CKM matrix effects can reduce the branching ratio of specific channels we considered, thereby affecting the associated bounds on the leptoquark parameter space. We have also not performed a full next-to-leading order simulation of the leptoquark pair production cross sections. These effects can be accounted for with available tools but would only affect quantitative aspect of our study without compromising our main message.
- It is important to note that all leptoquark scenarios that we presented require individual attention if one is to extract accurate parameter space constraints. In fact, even in the small Yukawa coupling limit, different scenarios would usually yield different lower bounds on the mass of relevant leptoquark(s). Our study should thus be seen as a blueprint for inclusion of the asymmetric leptoquark pair production effects and proper interpretation of available experimental data.

3 Atomic parity violation

In the proceeding section we produce leptoquark pair production search limits for various scalar leptoquark scenarios when the leptoquarks in question exclusively couple to either electrons or muons and the first generation quarks. In the former case it is also important to address the impact of the APV search constraints on otherwise viable leptoquark parameter space.

The effective APV interactions can be parametrized as [38]

$$\mathcal{L}_{\text{PV}} = \frac{G_F}{\sqrt{2}} (\bar{e}\gamma^\mu\gamma^5 e) \left(\sum_{q=u,d} \hat{C}_{1q} \bar{q}\gamma_\mu q \right), \quad (3.1)$$

where coefficients $\hat{C}_{1q} = C_{1q}^{\text{SM}} + C_{1q}^{\text{NP}}$ capture both the the SM and the New Physics (NP) contributions. In particular, $C_{1u}^{\text{SM}} = -0.1887$ and $C_{1d}^{\text{SM}} = 0.3419$ [39], whereas the NP contributions C_{1q}^{NP} for our scenarios are given in Table 5 [40, 41].

Non-zero Yukawas	C_{1u}^{NP}	C_{1d}^{NP}	LQ scenario
$y_{11}^{\text{LL}} \equiv y$	$-\frac{v^2}{4m_{\text{LQ}}^2} y ^2$	0	S_1
$y_{11}^{\text{RR}} \equiv y$	$\frac{v^2}{4m_{\text{LQ}}^2} y ^2$	0	
$y_{21}^{\text{LR}} \equiv y$	$-\frac{v^2}{4m_{\text{LQ}}^2} y ^2$	$-\frac{v^2}{4m_{\text{LQ}}^2} y ^2$	R_2
$y_{21}^{\text{RL}} \equiv y$	$\frac{v^2}{4m_{\text{LQ}}^2} y ^2$	0	
$y_{11}^{\text{RR}} = y_{21}^{\text{LR}} \equiv y$	0	$-\frac{v^2}{4m_{\text{LQ}}^2} y ^2$	$S_1 + R_2$
$y_{31}^{\text{LL}} \equiv y$	$-\frac{v^2}{4m_{\text{LQ}}^2} y ^2$	$-\frac{v^2}{2m_{\text{LQ}}^2} y ^2$	S_3
$y_{11}^{\text{LL}} = y_{31}^{\text{LL}} \equiv y$	$-\frac{v^2}{2m_{\text{LQ}}^2} y ^2$	$-\frac{v^2}{2m_{\text{LQ}}^2} y ^2$	$S_1 + S_3$

Table 5. C_{1q}^{NP} coefficients [40, 41] for the scalar leptoquark scenarios under consideration. The mass and Yukawa coupling degeneracies of leptoquarks are understood while $v = 246$ GeV.

The content of Table 5 clearly shows that each leptoquark scenario, except for the S_1 scenario with $y_{11}^{\text{RR}} \equiv y$ and R_2 with $y_{21}^{\text{RL}} \equiv y$ that are identical, is to be treated differently when it comes to APV constraints. This situation exactly mirrors our findings with regard to constraints originating from the leptoquark pair production search. We accordingly have six distinct cases to consider, all in all.

To proceed one defines a nuclear weak charge

$$Q_W(Z, N) = -2(2Z + N)2\hat{C}_{1u} - 2(Z + 2N)\hat{C}_{1d}, \quad (3.2)$$

where Z is a nuclear charge number and N represents a number of neutrons. The experimental measurements of the nuclear weak charge of the proton ($Q_W(p)$) and ^{133}Cs ($Q_W(^{133}\text{Cs})$) are [41, 42]

$$Q_W(p) = -2(2\hat{C}_{1u} + \hat{C}_{1d}) = 0.0719 \pm 0.0045, \quad (3.3)$$

and

$$Q_W(^{133}\text{Cs}) = -2(188\hat{C}_{1u} + 211\hat{C}_{1d}) = -72.82 \pm 0.42, \quad (3.4)$$

respectively. It is important to note that the measurement of $Q_W(p)$ is in agreement with the SM prediction whereas the measured value of $Q_W(^{133}\text{Cs})$ is not. In fact, the

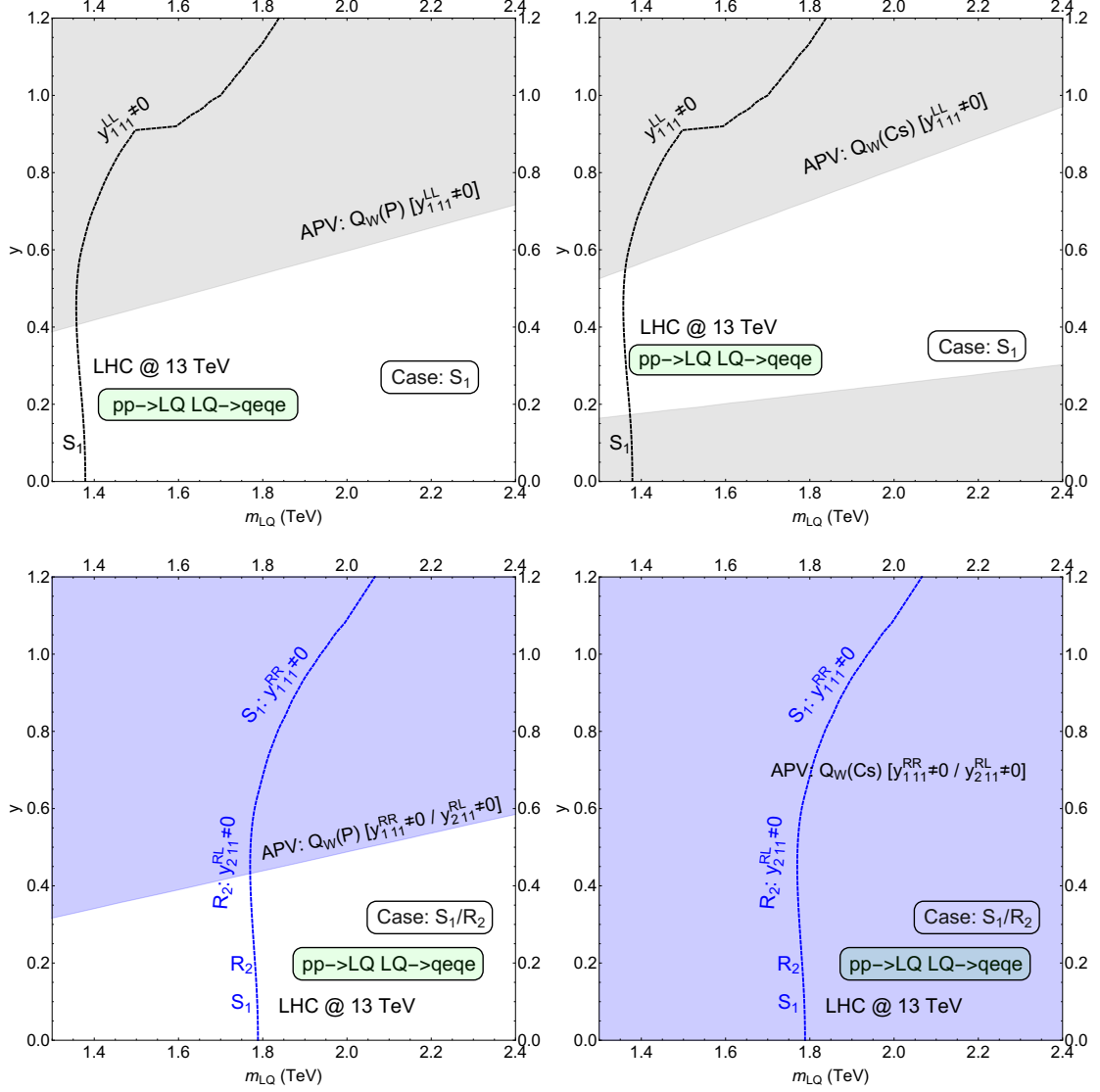


Figure 11. APV limits for the proton (left) and Cs (right) measurements juxtaposed with the leptoquark pair production search limits for the corresponding leptoquark scenarios, as indicated. Shaded regions are ruled out by the APV measurements.

value of $Q_W(^{133}\text{Cs})$ prefers finite negative NP contributions, as, for example, given with negative entries in Table 5. We accordingly opt to show separately constraints generated by measurements of $Q_W(p)$ and $Q_W(^{133}\text{Cs})$ in Figs. 11, 12, and 13, juxtaposing them with the leptoquark pair production search limits, where we also group aforementioned six different leptoquark scenarios pairwise. The first column in Figs. 11, 12, and 13 is reserved for the $Q_W(p)$ generated constraint, whereas the second column reflect the impact of the $Q_W(^{133}\text{Cs})$ measurement on the leptoquark parameter space. The shaded regions in Figs. 11, 12, and 13 are ruled out by the APV measurements at the 1σ level, where different leptoquark scenarios are shown in separate rows for clarity.

Fig. 13 clearly shows that the pair production constraint for the S_1+R_2 scenario is

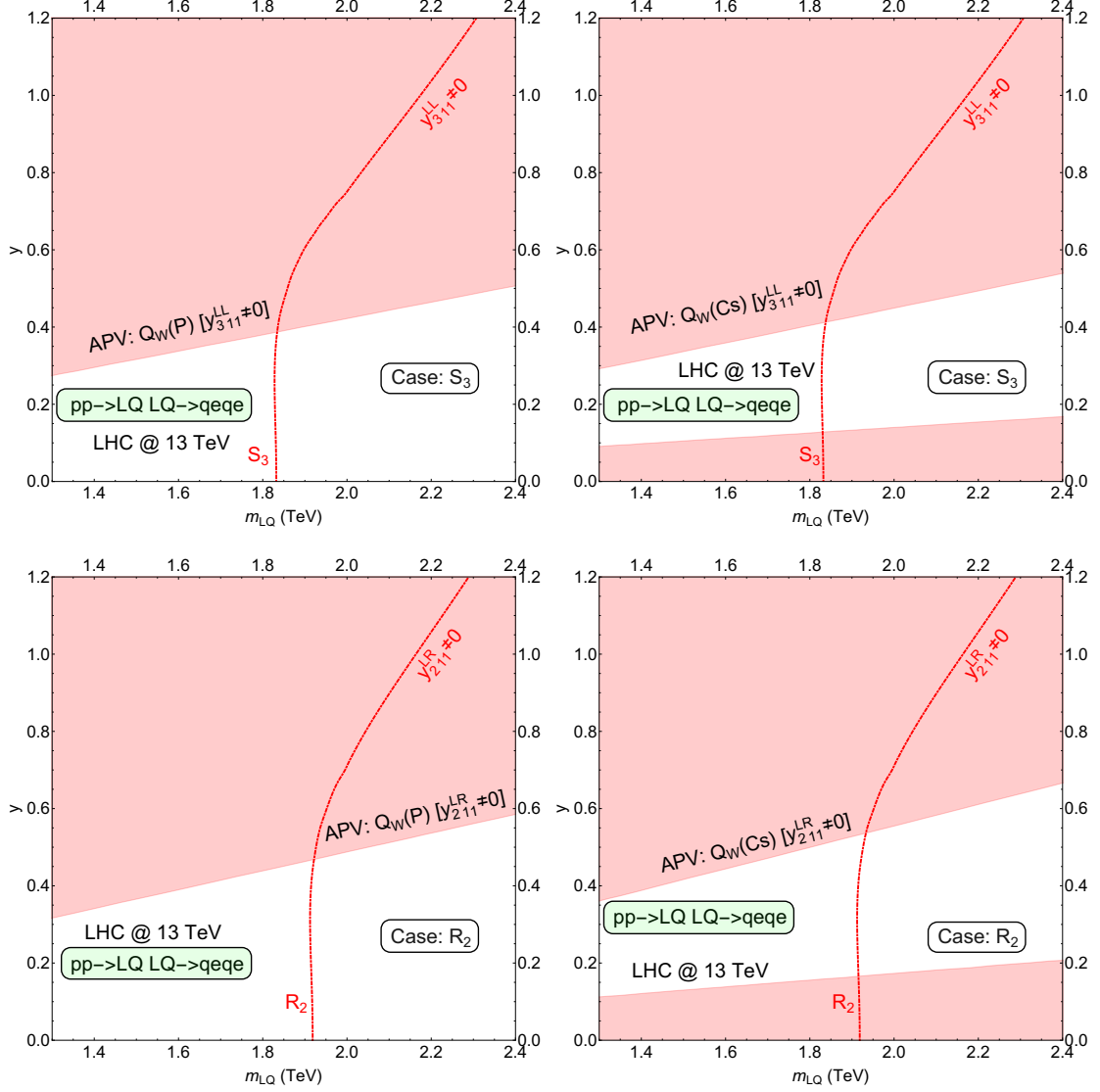


Figure 12. APV limits for the proton (left) and Cs (right) measurements juxtaposed with the leptoquark pair production search limits for the corresponding leptoquark scenarios, as indicated. Shaded regions are ruled out by the APV measurements.

superior to the existing APV constraints. It is also clear that the the S_1 scenario with $y_{111}^{\text{RR}} \neq 0$ and R_2 with $y_{211}^{\text{RL}} \neq 0$ are completely ruled out by the $Q_W(^{133}\text{Cs})$ measurement. Of course, the APV constraints are irrelevant for the scenarios when leptoquarks couple to muons. We also note that it is possible to arrange for cancellation between individual leptoquark contributions towards APV interactions of Eq. (3.1). This possibility of having the NP coefficients C_{1q}^{NP} vanish can be, for example, trivially realised within the S_1 scenario with $y_{111}^{\text{LL}} = y_{111}^{\text{RR}} \equiv y$ or within the $S_1 + R_2$ scenario with $y_{111}^{\text{LL}} = y_{211}^{\text{RL}} \equiv y$.

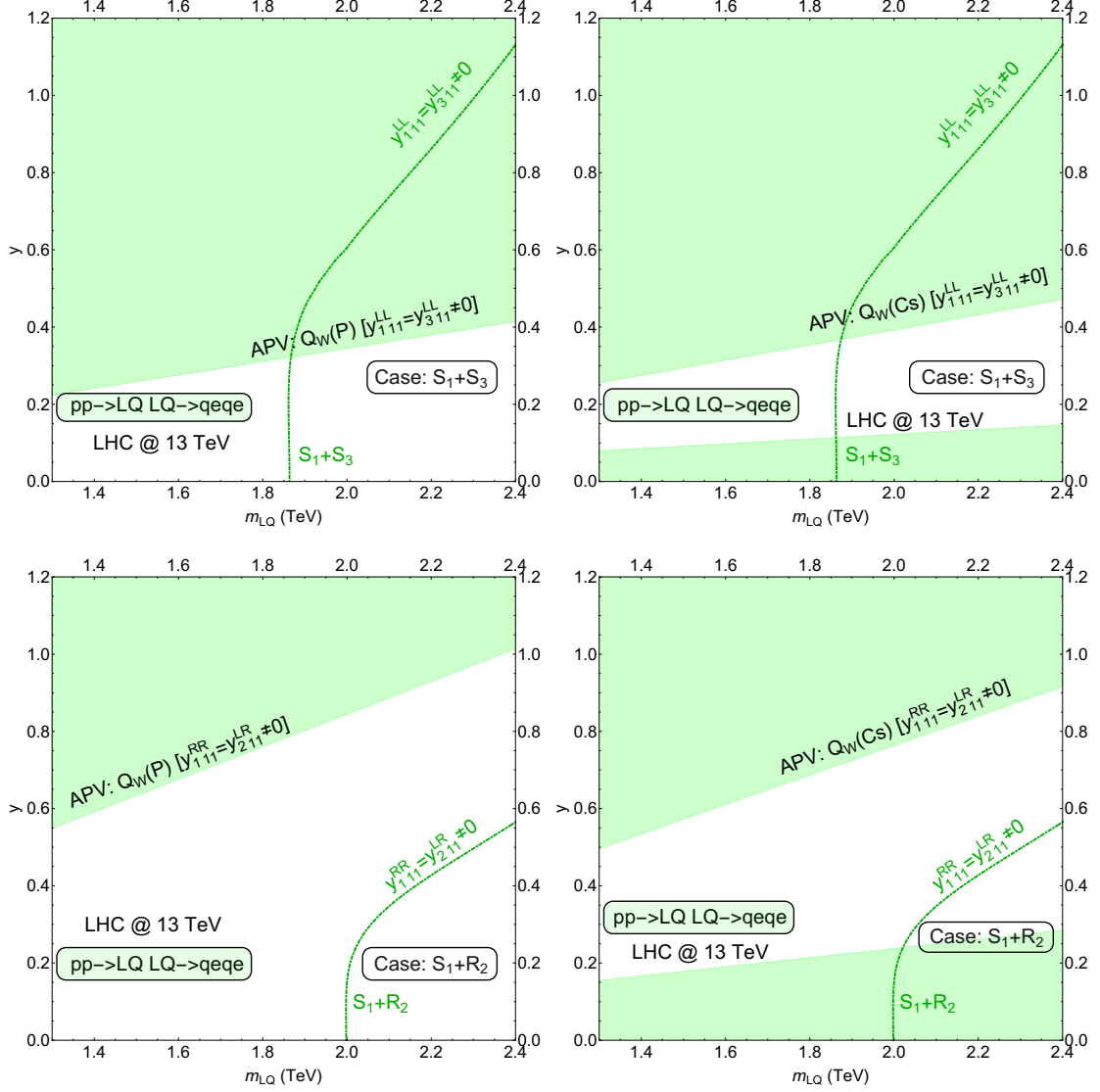


Figure 13. APV limits for the proton (left) and Cs (right) measurements juxtaposed with the leptoquark pair production search limits for the corresponding leptoquark scenarios, as indicated. Shaded regions are ruled out by the APV measurements.

4 Conclusions

This work investigates the asymmetric leptoquark pair production mechanism at the LHC. A sharp difference between the conventional leptoquark pair production and the asymmetric one is that for the latter, which is produced via t -channel lepton exchange, the pairs of produced leptoquarks are not conjugate states of each other. We spell out necessary conditions for an operational asymmetric leptoquark pair production mechanism and catalog all possible combinations of leptoquark multiplets that can potentially generate it. We, furthermore, demonstrate how to properly combine asymmetric and conventional pair production mechanism effects by considering several scenarios where the SM is extended with

either one or two scalar leptoquark multiplets. Finally, based on our analysis, we advocate that contributions from asymmetric pair production should be included when deriving reliable constraints on leptoquark parameter space as well as be used when attempting to perform correct identification of these promising new physics sources.

Acknowledgments

I.D. would like to thank Svjetlana Fajfer for numerous fruitful discussions with regard to this project.

References

- [1] **ATLAS** Collaboration, G. Aad *et al.*, “Search for pairs of scalar leptoquarks decaying into quarks and electrons or muons in $\sqrt{s} = 13$ TeV pp collisions with the ATLAS detector,” *JHEP* **10** (2020) 112, [arXiv:2006.05872 \[hep-ex\]](#).
- [2] **ATLAS** Collaboration, G. Aad *et al.*, “Search for pair production of scalar leptoquarks decaying into first- or second-generation leptons and top quarks in proton–proton collisions at $\sqrt{s} = 13$ TeV with the ATLAS detector,” *Eur. Phys. J. C* **81** no. 4, (2021) 313, [arXiv:2010.02098 \[hep-ex\]](#).
- [3] **CMS** Collaboration, A. M. Sirunyan *et al.*, “Search for singly and pair-produced leptoquarks coupling to third-generation fermions in proton-proton collisions at $s=13$ TeV,” *Phys. Lett. B* **819** (2021) 136446, [arXiv:2012.04178 \[hep-ex\]](#).
- [4] **ATLAS** Collaboration, G. Aad *et al.*, “Search for pair production of third-generation scalar leptoquarks decaying into a top quark and a τ -lepton in pp collisions at $\sqrt{s} = 13$ TeV with the ATLAS detector,” *JHEP* **06** (2021) 179, [arXiv:2101.11582 \[hep-ex\]](#).
- [5] **CMS** Collaboration, “The search for a third-generation leptoquark coupling to a τ lepton and a b quark through single, pair and nonresonant production at $\sqrt{s} = 13$ TeV,”.
- [6] M. Kramer, T. Plehn, M. Spira, and P. M. Zerwas, “Pair production of scalar leptoquarks at the Tevatron,” *Phys. Rev. Lett.* **79** (1997) 341–344, [arXiv:hep-ph/9704322](#).
- [7] M. Kramer, T. Plehn, M. Spira, and P. M. Zerwas, “Pair production of scalar leptoquarks at the CERN LHC,” *Phys. Rev. D* **71** (2005) 057503, [arXiv:hep-ph/0411038](#).
- [8] T. Mandal, S. Mitra, and S. Seth, “Pair Production of Scalar Leptoquarks at the LHC to NLO Parton Shower Accuracy,” *Phys. Rev. D* **93** no. 3, (2016) 035018, [arXiv:1506.07369 \[hep-ph\]](#).
- [9] I. Doršner and A. Greljo, “Leptoquark toolbox for precision collider studies,” *JHEP* **05** (2018) 126, [arXiv:1801.07641 \[hep-ph\]](#).
- [10] W. Beenakker, C. Borschensky, M. Krämer, A. Kulesza, and E. Laenen, “NNLL-fast: predictions for coloured supersymmetric particle production at the LHC with threshold and Coulomb resummation,” *JHEP* **12** (2016) 133, [arXiv:1607.07741 \[hep-ph\]](#).
- [11] W. Beenakker, M. Kramer, T. Plehn, M. Spira, and P. M. Zerwas, “Stop production at hadron colliders,” *Nucl. Phys. B* **515** (1998) 3–14, [arXiv:hep-ph/9710451](#).
- [12] W. Beenakker, S. Brensing, M. Kramer, A. Kulesza, E. Laenen, and I. Niessen, “Supersymmetric top and bottom squark production at hadron colliders,” *JHEP* **08** (2010) 098, [arXiv:1006.4771 \[hep-ph\]](#).

- [13] W. Beenakker, C. Borschensky, R. Heger, M. Krämer, A. Kulesza, and E. Laenen, “NNLL resummation for stop pair-production at the LHC,” *JHEP* **05** (2016) 153, [arXiv:1601.02954 \[hep-ph\]](#).
- [14] C. Borschensky, B. Fuks, A. Kulesza, and D. Schwartzländer, “Scalar leptoquark pair production at hadron colliders,” *Phys. Rev. D* **101** no. 11, (2020) 115017, [arXiv:2002.08971 \[hep-ph\]](#).
- [15] A. Alves, O. Eboli, and T. Plehn, “Stop lepton associated production at hadron colliders,” *Phys. Lett. B* **558** (2003) 165–172, [arXiv:hep-ph/0211441](#).
- [16] I. Dorsner, S. Fajfer, and A. Greljo, “Cornering Scalar Leptoquarks at LHC,” *JHEP* **10** (2014) 154, [arXiv:1406.4831 \[hep-ph\]](#).
- [17] J. B. Hammett and D. A. Ross, “NLO Leptoquark Production and Decay: The Narrow-Width Approximation and Beyond,” *JHEP* **07** (2015) 148, [arXiv:1501.06719 \[hep-ph\]](#).
- [18] T. Mandal, S. Mitra, and S. Seth, “Single Productions of Colored Particles at the LHC: An Example with Scalar Leptoquarks,” *JHEP* **07** (2015) 028, [arXiv:1503.04689 \[hep-ph\]](#).
- [19] M. Schmaltz and Y.-M. Zhong, “The leptoquark Hunter’s guide: large coupling,” *JHEP* **01** (2019) 132, [arXiv:1810.10017 \[hep-ph\]](#).
- [20] D. A. Faroughy, A. Greljo, and J. F. Kamenik, “Confronting lepton flavor universality violation in B decays with high- p_T tau lepton searches at LHC,” *Phys. Lett. B* **764** (2017) 126–134, [arXiv:1609.07138 \[hep-ph\]](#).
- [21] N. Raj, “Anticipating nonresonant new physics in dilepton angular spectra at the LHC,” *Phys. Rev. D* **95** no. 1, (2017) 015011, [arXiv:1610.03795 \[hep-ph\]](#).
- [22] A. Greljo and D. Marzocca, “High- p_T dilepton tails and flavor physics,” *Eur. Phys. J. C* **77** no. 8, (2017) 548, [arXiv:1704.09015 \[hep-ph\]](#).
- [23] S. Bansal, R. M. Capdevilla, A. Delgado, C. Kolda, A. Martin, and N. Raj, “Hunting leptoquarks in mono-lepton searches,” *Phys. Rev. D* **98** no. 1, (2018) 015037, [arXiv:1806.02370 \[hep-ph\]](#).
- [24] J. Fuentes-Martin, A. Greljo, J. Martin Camalich, and J. D. Ruiz-Alvarez, “Charm physics confronts high- p_T lepton tails,” *JHEP* **11** (2020) 080, [arXiv:2003.12421 \[hep-ph\]](#).
- [25] L. Allwicher, D. A. Faroughy, F. Jaffredo, O. Sumensari, and F. Wilsch, “Drell-Yan Tails Beyond the Standard Model,” [arXiv:2207.10714 \[hep-ph\]](#).
- [26] J. Ohnemus, S. Rudaz, T. F. Walsh, and P. M. Zerwas, “Single leptoquark production at hadron colliders,” *Phys. Lett. B* **334** (1994) 203–207, [arXiv:hep-ph/9406235](#).
- [27] O. J. P. Eboli, R. Zukanovich Funchal, and T. L. Lungov, “Signal and backgrounds for leptoquarks at the CERN LHC,” *Phys. Rev. D* **57** (1998) 1715–1729, [arXiv:hep-ph/9709319](#).
- [28] L. Buoncore, U. Haisch, P. Nason, F. Tramontano, and G. Zanderighi, “Lepton-Quark Collisions at the Large Hadron Collider,” *Phys. Rev. Lett.* **125** no. 23, (2020) 231804, [arXiv:2005.06475 \[hep-ph\]](#).
- [29] A. Greljo and N. Selimovic, “Lepton-Quark Fusion at Hadron Colliders, precisely,” *JHEP* **03** (2021) 279, [arXiv:2012.02092 \[hep-ph\]](#).

- [30] L. Buonocore, A. Greljo, P. Krack, P. Nason, N. Selimovic, F. Tramontano, and G. Zanderighi, “Resonant leptoquark at NLO with POWHEG,” [arXiv:2209.02599 \[hep-ph\]](#).
- [31] I. Doršner, S. Fajfer, and A. Lejlić, “Novel Leptoquark Pair Production at LHC,” [arXiv:2103.11702 \[hep-ph\]](#).
- [32] C. Borschensky, B. Fuks, A. Jueid, and A. Kulesza, “Scalar leptoquarks at the LHC and flavour anomalies: a comparison of pair-production modes at NLO-QCD,” [arXiv:2207.02879 \[hep-ph\]](#).
- [33] I. Doršner, S. Fajfer, A. Greljo, J. F. Kamenik, and N. Košnik, “Physics of leptoquarks in precision experiments and at particle colliders,” *Phys. Rept.* **641** (2016) 1–68, [arXiv:1603.04993 \[hep-ph\]](#).
- [34] A. Alloul, N. D. Christensen, C. Degrande, C. Duhr, and B. Fuks, “FeynRules 2.0 - A complete toolbox for tree-level phenomenology,” *Comput. Phys. Commun.* **185** (2014) 2250–2300, [arXiv:1310.1921 \[hep-ph\]](#).
- [35] J. Alwall, R. Frederix, S. Frixione, V. Hirschi, F. Maltoni, O. Mattelaer, H. S. Shao, T. Stelzer, P. Torrielli, and M. Zaro, “The automated computation of tree-level and next-to-leading order differential cross sections, and their matching to parton shower simulations,” *JHEP* **07** (2014) 079, [arXiv:1405.0301 \[hep-ph\]](#).
- [36] NNPDF Collaboration, R. D. Ball *et al.*, “Parton distributions for the LHC Run II,” *JHEP* **04** (2015) 040, [arXiv:1410.8849 \[hep-ph\]](#).
- [37] C. Borschensky, B. Fuks, A. Kulesza, and D. Schwartländer, “Scalar leptoquark pair production at the LHC: precision predictions in the era of flavour anomalies,” [arXiv:2108.11404 \[hep-ph\]](#).
- [38] P. Langacker, “Parity violation in muonic atoms and cesium,” *Phys. Lett. B* **256** (1991) 277–283.
- [39] Qweak Collaboration, D. Androić *et al.*, “Precision measurement of the weak charge of the proton,” *Nature* **557** no. 7704, (2018) 207–211, [arXiv:1905.08283 \[nucl-ex\]](#).
- [40] V. D. Barger and K.-m. Cheung, “Atomic parity violation, leptoquarks, and contact interactions,” *Phys. Lett. B* **480** (2000) 149–154, [arXiv:hep-ph/0002259](#).
- [41] A. Crivellin, D. Müller, and L. Schnell, “Combined constraints on first generation leptoquarks,” *Phys. Rev. D* **103** no. 11, (2021) 115023, [arXiv:2104.06417 \[hep-ph\]](#). [Addendum: *Phys.Rev.D* 104, 055020 (2021)].
- [42] Particle Data Group Collaboration, P. A. Zyla *et al.*, “Review of Particle Physics,” *PTEP* **2020** no. 8, (2020) 083C01.